Coordination Chemistry Reviews, 110 (1991) 161–210
Elsevier Science Publishers B.V., Amsterdam

METAL NMR OF ORGANOMETALLIC (d-BLOCK) SYSTEMS

DIETER REHDER
Institut für Anorganische und Angewandte Chemie, Universität Hamburg, 2000 Hamburg 13 (F.R.G.)

(Received 3 January 1991)

CONTENTS

ABBREVIATIONS

Ac	Acetate
acac	acetylacetonate(1-)
bipy	2,2′-bipyridine
Bu, *s*Bu, *t*Bu	butyl, sec-butyl, tert-butyl
COD	cyclooctadiene
COT	cyclooctatetraene
Cp	η^5-C_5H_5, if not indicated otherwise
Cp′	η^5-C_5H_4Me

0010-8545/91/$17.50

Cp*	η^5-C_5Me_5
dppm, dppe, dppb	$Ph_2P(CH_2)_nPPh_2$: $n = 1, 2, 4$
diars	*o*-phenylenebis(dimethylarsine)
Ind	η^5-indenyl
Me	methyl
Mes	mesityl (1,3,5-trimethylphenyl)
nor	norbornadiene
NQCC	nuclear quadrupole coupling constant
Ph	phenyl
pyr	pyridine
Pr	propyl
THF (thf)	tetrahydrofurane (coordinated)
tol	tolyl
$W_{1/2}$	line width at half-height

A. INTRODUCTION

NMR techniques carried out in the periphery, i.e. in the organic moiety of an organometallic compound have been widely and successfully applied to elucidate structures, dynamic behaviour, chemical exchange processes and the like. The nuclei probed are usually ^1H and ^{13}C, hence nuclei for which extensive data bases, well-established and sophisticated measuring techniques, and analytical tools for interpreting the spectra exist. ^1H (and also ^{19}F and ^{31}P; X) have also been used to obtain information on the metal (M) nucleus, such as scalar coupling constants $J(X-M)$ and metal chemical shifts $\delta(M)$, mainly where the nuclear properties of the metal nucleus are unfavourable for direct methods (e.g. low magnetogyric ratio, low natural abundance, very long relaxation times). There are many examples in the literature of this indirect evaluation of metal nuclei by methods known as, for example, DEPT, INEPT, and 2D(X,M). The interested reader might consult refs. 1 and 2 for details. Metal NMR data obtained from indirect methods will be considered in this review only where other material is not available or is needed for comparative discussions.

NMR parameters directly obtained from the coordination centre, i.e. by probing the metal nucleus itself, may provide more appropriate information. This is the case, for example, when electronic properties are probed in a context of chemical reactivity or catalytic activity of an organometallic compound. This is also true when it comes to parametrization of NMR observables with respect to even subtle stereo-electronic changes in the ligand sphere. Finally, metal NMR turns out to be advantageous in carrying out unambiguous speciation in a complex reaction pattern or in a multi-site (cluster) compound.

The most prominant gain of metal NMR with respect to ^1H NMR comes from the greater intrinsic sensitivity of the former, i.e. a shielding range larger, in many cases, by orders of magnitude. Variations in transition metal shielding, owing to the

presence of d orbitals (also in the d^0 cases these are involved in bonding), are governed by d contributions to the paramagnetic term of the overall shielding tensor (vide infra), while diamagnetic contributions are dominated by the core electrons and hence are constant to a first approximation [3–9]. This makes interpretation of variations in chemical shifts more complex than, e.g. in ^{1}H or ^{13}C NMR, but may increase the amount of information that can be extracted from this sensitive parameter.

As a consequence, direct metal NMR investigations have been carried out for a variety of nuclei, some having suitable nuclear properties, quite extensively. Several monographs have appeared for the latter (^{51}V [10], ^{95}Mo and ^{183}W [11], ^{195}Pt [12]). In addition, reviews [3–7], including theoretical aspects [8,9], and books [13–15], covering the field have been published; none of these, however, concentrates on organometallics. The rapidly developing improvement of instrumentation has made the more difficult nuclei (such as $^{47,49}Ti$, ^{53}Cr, ^{89}Y, ^{91}Zr, ^{99}Ru, ^{103}Rh, ^{139}La, ^{171}Yb, ^{189}Os) increasingly accessible to direct observation, and these will be addressed specifically in the present review, together with a comprehensive selection of the (mostly) more recent results for metal nuclei less problematic or more commonly probed in NMR experiments (^{51}V, ^{55}Mn, ^{57}Fe, ^{59}Co, ^{93}Nb, ^{95}Mo, ^{113}Cd, ^{183}W, ^{195}Pt and ^{199}Hg). Most of the d-block nuclei have quadrupole moments Q (i.e. a non-spherical distribution of the nuclear charge), giving rise to very effective relaxation, often referred to as quadrupole relaxation, and hence broad lines. Among these, only ^{51}V and ^{95}Mo have sufficiently small values of Q (-0.052 and -0.019×10^{-28} M^2, respectively) to provide sufficiently sharp resonance lines even in complexes where there is virtually no symmetry. In all other cases, one is usually restricted to systems of cubic point symmetry and several other cases [16] where quadrupole relaxation becomes small or ineffective. The spin 1/2 nuclei among the d-block metals are ^{57}Fe, ^{89}Y, ^{103}Rh, $^{107,109}Ag$, ^{111}Cd, ^{171}Yb, ^{183}W, ^{187}Os, ^{195}Pt and ^{199}Hg.

The treatment of data in this review will follow the mode of metal–carbon interaction in the organometallic compound, and within this classification, along the vertical groups in the Periodic Table. Carbonyl and isonitrile complexes will not be considered as such but only where organic ligands are coordinated in addition to CO. Where more than one class of carbon ligands is attached to a metal, priority in treatment follows the classification given in the Contents. For example, the reader will find η^5-$C_5H_5Mo(CO)_3CH_3$ under σ-alkyl complexes (Sect. B), $[\eta^5$-$C_5H_5Mo(CO)_3]^-$ under π-arene complexes (Sect. E). If σ- and π-bonded Cp is present, the compounds are listed with π—Cp complexes. Compounds containing the fulvene ligand, including those for which a (η^5, σ) coordination has been established, are discussed in the context of π-arene complexes. η^4-Cyclobutadiene is considered an aromatic ligand (i.e. $C_4H_4^{2-}$).

Many of the more general aspects of metal shielding, such as the effects imparted by ligand electronegativity and polarizability, σ donor/π acceptor ability, steric effects (ligand bulkiness, chelate-ring size), substituent effects, and effects of local symmetry

will be dealt with in Sect. B, mainly in the context of ^{51}V (i) and ^{195}Pt NMR (iv), where a sufficiently large amount of data on organovanadium and organoplatinum compounds is available for a study of trends.

^{171}Y, the only f-block element for which NMR data in an organometallic environment exist (La is considered here a d-block metal), is included in this report.

The question of standards in NMR measurements (and references for the chemical shift scales) sometimes appears to be a tedious one. While, for most nuclei, there is general agreement on the standard (which is usually identical to what is used as the zero point of the δ scale), several standards/references exist for most of the platinum metals. Thus, for ^{103}Rh, three scales to reference $\delta(^{103}Rh)$ values have been used in the literature, based on (i) an arbitrary standard with $\nu(Rh)/\nu(TMS)=0.0316$ ($\Xi=3.16$ MHz), (ii) Rh metal, and (iii) saturated $Rh(acac)_3$ in $CDCl_3$. The last of these, which is a practicable standard in ^{103}Rh NMR, has been employed by Benn and co-workers, and is used as the reference in this review. Data from other sources have been adapted to this scale, employing the reported shift values for (acac)Rh(1,3-COD) (−7014 ppm) [2]; Rh metal (+2680 ppm) [17] and $\Xi=3.16$ MHz (+1294) [18]. Similarly, various scales have been used for referencing $\delta(^{195}Pt)$, among these $\Xi(^{195}Pt)=21.4$ MHz, and $[PtCl_6]^{2-}$. Although the standard employed in direct measurements is usually hexachloroplatinate (or H_2PtCl_6), I have adapted, in this review, to the $\Xi=21.4$ MHz scale, yielding to an increasing trend towards absolute shift scales. $\delta(^{195}Pt[PtCl_6^{2-}/H_2O])=+4522$ ppm relative to $\Xi(^{195}Pt)$ as the zero point has been used for recalculations. $\delta(^{57}Fe)$ values in this review are quoted relative to the now accepted $\delta[Fe(CO)_5$ neat$]=0$ scale ($\delta[Fe(CO)_5/CS_2]=+21$ ppm). $\delta(^{57}Fe)$ reported relative to ferrocene have been recalculated, based on $\delta[FeCp_2/CS_2]=+1560$ and $\delta[FeCp_2/THF]=+1534$ ppm. For a more detailed discussion of the referencing problems see, for example, Goodfellow in ref. 14 and Granger in ref. 13. The reference points employed here are summarized in Table 1.

Higher shielding of a metal nucleus in a compound A with respect to a compound B will be quoted as "upfield shift" throughout, where "upfield" refers to higher magnetic field (lower frequency). Hence δ_A is less positive or more negative than δ_B.

B. COMPLEXES CONTAINING AN M–C_σ(sp, sp^2 OR sp^3) BOND

In this section, σ-alkyl, -aryl, -alkenyl, -vinyl and -alkynyl compounds, carbenes and carbynes will be treated. Metallacycles are included.

(i) Alkyl and related complexes of Groups 3–5

With the exception of vanadium, for which a sufficiently large amount of material is available, which allows for comparative studies, the NMR data of alkyl and related complexes of the early transition metals (Table 2) have only been reported

TABLE 1

References ($\delta = 0$) used for the data listings and text discussions in this review

Nucleus	Reference ($\delta = 0$)
^{49}Ti	$TiCl_4$ neat
^{51}V	$VOCl_3$ neat or dissolved in $CDCl_3$
^{53}Cr, ^{95}Mo, ^{183}W	Aqueous $[MO_4]^-$, 1–2 M, pH ca. 12
^{55}Mn	$K[MnO_4]$, saturated aqueous solution
^{57}Fe	$Fe(CO)_5$ neat
^{59}Co	Aqueous $K_3[Co(CN)_6]$
^{45}Sc, ^{89}Y, ^{135}La	M^{3+} (preferably $M[ClO_4]_3$) in water, ca. 1 M = $[M(H_2O)_6]^{3+}$ ($\rightleftharpoons [M(H_2O)_5OH]^{2+}$)
^{91}Zr	Cp_2ZrBr_2 in THF
^{93}Nb	$NbCl_5 + [Et_4N]Cl$ in abs. MeCN = $[Et_4N][NbCl_6]$
^{103}Rh	$Rh(acac)_3$, saturated in $CDCl_3$
^{113}Cd	$CdMe_2$ neat
^{171}Yb	$Cp^*_2Yb(thf)_2$ in THF
^{187}Os	OsO_4
^{195}Pt	$\nu(^{195}Pt)/\nu(^1H[TMS]) = 0.0214$, i.e. $\Xi(^{195}Pt) = 21.4$ MHz
^{199}Hg	$HgMe_2$ neat

sporadically. Among these are ^{89}Y shift values for two methyl complexes from the only direct ^{89}Y NMR study of organoyttrium compounds [19]. The two signals observed in the ^{139}La NMR of the anion $[Cp_3LaBu]^-$ have been attributed to slow equilibria as given in eqn. (1) [20], the broad lines to fast chemical exchange as shown in eqn. (2). This equilibrium has been verified by ^{139}La–^{139}La exchange spectroscopy (2D-EXSY) [21].

$$2[Cp_3LaBu]^- \rightleftharpoons [\{Cp_3La\}_2\mu\text{-}Bu]^- + Bu^- \quad (1)$$

$$[Cp_3La^*Bu]^- + [Cp_3LaBu^*]^- \rightleftharpoons [Cp_3La^*Bu\ ^*]^- + [Cp_3LaBu]^- \quad (2)$$

^{51}V shielding may decrease or increase with the increasing bulk of a substituent (ligand) R. An increase is noted (Table 2) for the series **2** ($Me < CH_2tBu < CH_2SiMe_3$) and **5** ($tBu > iPr > Me$), a decrease for **1** ($tBu < sBu < nBu$). The fact that opposite effects are observed in the two d^0 (closed shell) series **1** and **2** demonstrates the complex nature of the steric effect.

Replacing alkoxide or chloride by alkyls leads to a quite substantial deshielding of the ^{51}V nucleus in the $V^{(V)}$ complexes **3** and **4**. σ-Bonded carbon functions can be classified as soft, i.e. easily polarizable ligands, and as such impart, in d^0 systems, low shielding (inverse polarizability dependence). σ-Alkyls exert a shielding effect similar to that of bromide, and are placed in the following series of increasing shielding contributions: $\{Se\} < \{S\} < \sigma\text{-alkyl} \approx Br < Cl < \{N\} \approx \{O\} < F$. $\{E\}$ symbolizes a ligand coordinating via its function E, e.g. $\{O\} = OR^-, O^{2-}, OC(O)^-$ etc.

The electronically induced trends can be traced back to the paramagnetic

TABLE 2

Data for alkyl complexes of metals of Groups 3–5

Compound	δ(M) (ppm)	$W_{1/2}$ (Hz)	Ref.
$Cp'_2Y(Me)THF$	+40		19
$\{Cp'_2Y(\mu\text{-}Me)\}_2$	−15		19
$[Cp_3La(Bu)]^-$	−556; −526	750; 5,830	20
$MeTiCl_3$	+618	50	22
$MeTiBr_3$	+825	100	22
$Zr(tBu)_4$	+799	20	2
$Cp_2ZrCl(vinyl)$	+16	1250	23
$O{=}V(Cp^*)Ph_2$	−362		24
$tBuN{=}V(Cp)(NHtBu)R$ **1**			
R = Me	−754	310	25
*n*Bu	−682	320	25
*s*Bu	−617	410	25
*t*Bu	−566	370	25
$tBuN{=}V(Cp)(OtBu)mes$	−758	400	26
$tBuN{=}V(Cp)(OtBu)Me$	−706	320	26
$tBu_3SiN{=}V(HNSitBu_3)Cl(R)$ **2**			
R = Me	+570	230	29
CH_2tBu	+386	180	29
CH_2SiMe_3	+279	150	29
$RN{=}VX_{3-n}(CH_2SiMe_3)_n$			
X = O*t*Bu **3**			
R = *t*Bu, *n* = 1	−357[a]	270	27
n = 2	+242[a]	370	27
n = 3	+877[a]	240	27
X = Cl **4**			
R = tol, *n* = 1	+697	380	28
n = 2	+900	350	28
n = 3	+1048[a]	270	28
$Li[(tBu_3SiN)_2VMe_2]$	+417	220	29
$RV(CO)_4dppe$ **5**			
R = *t*Bu	−1096		30
iPr	−1048		30
Me	−1032		30

[a] $^1J(^{14}N\text{–}^{51}V)$ coupling resolved (86–101 Hz).

deshielding contribution σ'(para) of the overall shielding $\sigma' = \sigma'(dia) + \sigma'(para)$. I have mentioned already that the diamagnetic contribution is determined mainly by the core electrons and is therefore practically constant for a given nucleus. Hence, alterations in shielding are governed by the paramagnetic term which, in a rather

simplified but quite practicable version, may be represented by eqn. (3) (see, for example, ref. 8 for the exact treatment in the frame-work of Ramsey's equation):

$$\sigma'(\text{para}) = \text{const.}\ \overline{\Delta E^{-1}} \langle r^{-3} \rangle_{\text{val}} \overline{(C^2)_{\text{val}}} \qquad (3)$$

Here, $\overline{\Delta E}$ is the mean HOMO–LUMO gap, r_{val} the distance of the valence p and d electrons from the nucleus, and $\overline{C_{\text{val}}}$ the mean valence LCAO coefficient. As has been shown for the d^0 compounds $O{=}VX_3$ (X = Br, Cl, OR, F [15,31]) and $[MoO_{4-n}S_n]^{2-}$ [32], p electrons only play a secondary role (except for the post-transition metals; see Sect. B. (v)). There are substantial d contributions to the HOMOs, and d–d excitations are the dominant factors for changes in σ'. The increasing softness of X leads to (i) a decrease of the HOMO–LUMO gap and (ii) an increase of d character (increase of C_d) of the HOMO. Both effects point in the same direction, namely an increase of σ'(para), i.e. net deshielding. The observed low shielding in V–d^0 alkyls is in accord with this view.

(ii) Chromium, molybdenum and tungsten

The overall shift ranges for these three metals are $\delta = 0$ to -1800 for ^{53}Cr, $\delta = +4200$ to -2100 for ^{95}Mo, and $\delta = +6800$ to -4100 for ^{183}W, all relative to aqueous $[MO_4]^{2-}$. There are several technical problems involved in the routine measurement of the ^{53}Cr resonance, which include the small magnetic moment and a low receptivity. ^{53}Cr ($I = 3/2$) and ^{95}Mo ($I = 5/2$) have medium to small quadrupole moments (-0.15×10^{-28} and -0.019×10^{-28} m^2, respectively), ^{183}W is a spin 1/2 nucleus, usually with rather long relaxation times.

A single comprehensive study of organochromium compounds, dealing with pentacarbonylchromium carbene and isonitrile complexes, has appeared [33]. Selected data are listed in Table 3. ^{53}Cr shielding for 46 carbene complexes, somewhat less pronounced than in $Cr(CO)_6$ ($\delta = -1795$ ppm) but still clearly on the high-field side, spans a range of 214 ppm. Correlations have been established between ^{53}Cr shielding and the factor $\langle r^{-3} \rangle C^2$ (but not with ΔE) in eqn. (3), and the donor/acceptor properties of the carbenes have been discussed to explain the observed trends: two hetero atoms residing on the carbene carbon give rise to effective ^{53}Cr shielding as long as steric effects do not hamper optimal overlap conditions. While there is no corollary between ^{53}Cr shielding and the reactivity of the carbene complexes towards imines to form β-lactams (see eqn. (6) in Scheme 2), the line widths of the resonance signals appear to be related to reactivity.

For Mo and W, quadruply bonded $[M{\equiv}M]^{4+}$ complexes are at the low-field and carbonyl complexes at the high-field side. Other compounds fall within this range. In the $Mo^{(II)}$ complexes $CpMo(CO)_3(alkyl)$, the ^{95}Mo nucleus is more shielded than in the corresponding halide derivatives, but less than in the hydride ($\delta = -2047$) and stannyl compounds (-2072 ppm). In the benzyl complexes **6**, there is an apparent aryl substituent effect on $\delta(^{95}Mo)$ [35]. However, the data do not suffice to account

TABLE 3

Data for alkyl, carbene and carbyne complexes of Group 6 metals

Compound	δ(M)[a] (ppm)	$W_{1/2}$[b] (Hz)	Ref.
$(CO)_5Cr{=}CR(R')$			33
R = Me, R' = OMe	−1608	900	
NMeH *E*	−1659	800	
Z	−1702	750	
R = Ph, R' = OMe	−1550	1100	
R, R' = OMe	−1686	350	
R, R' = {N(Me)CH_2-}$_2$	−1739	280	
$CpMo(CO)_3Me$	−1736	40	34
$CpMo(CO)_3CH_2Mes$	−1599	60	35
$CpMo(CO)_3CH_2C_6H_4R$ **6**		40–70	35
R = 4-OMe	−1587		
3-OMe	−1574		
2-OMe	−1573		
4-Me	−1583		
4-F	−1577		
4-Cl	−1566		
$4CF_3$	−1551		
$(CO)_3W(X)\{CNN\}$ **7**[c]			36
X = F	−1411		
Cl	−1351		
Br	−1357		
I	−1413		
$M{\equiv}CSiMe_3(CH_2R)_3$ **8**[d]			37
R = $SiMe_3$	+1845; +3613[e]		
*t*Bu	+1400; +2867[e]		
$W{\equiv}CPh(OtBu)_3$	+2526		37
$Mo_2(CH_2R)_6$ **9**[d]			37
R = *t*Bu	+3695	530	
$SiMe_3$	+3625	530	
$M_2(CH_2tBu)_2(O_2CMe)_4$ **10**[d]	+2040; +2653	1460	37

[a] $\delta(^{53}Cr)$, $\delta(^{95}Mo)$ and $\delta(^{183}W)$, respectively, relative to aqueous $[MO_4]^{2-}$. $\delta(^{53}Cr)$ values have been recalculated from the data given in ref. 33 relative to $Cr(CO)_6$, using $\Delta\delta = 1795$ ppm. In cases where there are two entries for δ(M), the first refers to M = Mo, the second to M = W.

[b] Half-widths for the molybdenum complexes.

[c] See Scheme 1. $^3J(^1H{-}^{183}W) = 8$ Hz.

[d] See Scheme 1.

[e] Septet; $^2J(^1H{-}^{183}P) = 10.5$ Hz.

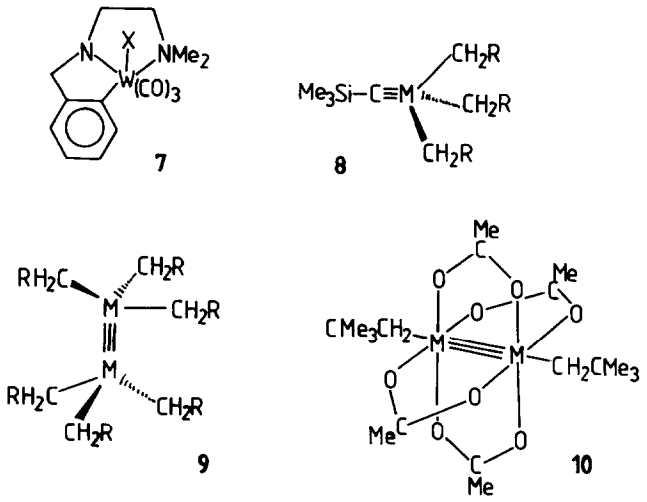

Scheme 1.

for a systematic trend. The $W^{(II)}$ metallacycles **7** (Scheme 1) exhibit, with the exception of the fluorine compound, the normal polarizability (normal halogen [36]) dependence of metal shielding commonly observed in low-valent transition metal complexes, where the softer (less electronegative) ligand gives rise to enhanced covalency of the metal–ligand bond and hence to a decrease of σ'(para) (via a decrease of C_{nd}) in eqn. (3). The fact that the fluorine derivative does not follow the trend may be due to a decrease of its effective electronegativity by hydrogen bond interctions. The data for the complexes **7** have been obtained via 2-D indirect (^{1}H,^{183}W) NMR spectroscopy. This detection scheme [38] allows efficient access to insensitive spin 1/2 nuclei (such as ^{183}W) when coupled to a sensitive one like ^{1}H or, as discussed in section (iv), ^{31}P.

The special bonding situation in the complexes **8** (with a metal–carbon triple bond) and **9** and **10** (with metal–metal triple bonds) gives rise to a rather unique deshielding situation for the nuclei ^{95}Mo and ^{183}W. ^{95}Mo shielding decreases in the sequence $[M{\equiv}CR]^{3+} > [M{\equiv}M]^{6+}$ ($\pi^4\delta^2$; **10**) $> [M{\equiv}M]^{6+}$ ($\sigma^2\pi^4$; **9**) and is only exceeded by quadruply bonded complexes. The reasons for the extreme deshielding are not clear. The resonances in the type **8** tungsten carbyne complexes are septets due to $^2J(^1H–^{183}W)$ coupling involving the six hydrogens of the alkyl groups.

$\delta(^{95}Mo)$ and $\delta(^{183}W)$ values are often related to each other in terms of a common ratio $\Delta\delta(^{183}W)/\Delta\delta(^{95}Mo)$, where $\Delta\delta$ refers to pairs of analogous complexes. This ratio, which, for diverse classes of Mo and W complexes, amounts to approximately 1.5 [39], is indicative of a higher intrinsic shielding sensitivity of the ^{183}W nucleus over that of the ^{95}Mo nucleus by a factor of ca. 1.5.

(iii) Manganese: correlations between chemical shifts, substituent effects and kinetic parameters

The manganese chemical shift [$\delta(^{55}Mn)$; Table 4], a molecular ground state parameter, has been shown to correlate with a kinetic parameter, the rate constant for the proton-induced demetallation reaction of the manganacycle **13a** [eqn. (5) in Scheme 2], in that rate constants are greater for the more effectively shielded ^{55}Mn nuclei [43]. Increased shielding in turn is observed with increased electron-donating ability of the substituent Z in **13a** as quantified by Hammett's σ constant, suggesting a relationship between electronic factors that control metal shielding and the energy of the transition state for demetallation [42].

An analogous trend has also been reported for the alkyl and acyl complexes **11** and **12** [40]. In both cases, these trends are again in accord with theoretical predictions [9], according to which shielding in an open-shell d system (low-valent metal complex) increases as the softness of the ligand increases. The substantial deshielding (with respect to **11** and **12**) in the manganacycles **13** and **14**, where a hard oxygen function participates in coordination, is in line with this normal polarizability dependence of metal shielding [Sect. B. (i)], but also reflects the decrease of shielding commonly observed as the degree of CO substitution increases.

Quite interestingly, $\delta(^{55}Mn)$ values may also be exploited to predict the reactivity of alkylcarbonylmanganese complexes towards migratory CO insertion [eqn. (4) in Scheme 2]: the higher the shielding, the more readily the acyl complex is formed. Manganese complexes that have $\delta(^{55}Mn)$ values less negative than -1900 are resistant to alkyl migration [42].

The complex **15**, a precursor to the η^3-allyl complex **36** (Sect. D) of $Mn(CO)_4$,

TABLE 4

NMR parameters of organomanganese (cf. Scheme 2) and related complexes

Compound	$\delta(^{55}Mn)$ (ppm)	$W_{1/2}$ (kHz)	Ref.
$(CO)_5MnX$, X = H	−2630	2.6	3
CH_3	−2265	3.0	3
$CH_2C_6H_4Z$ **11a**	−2040 to −1989	4–5	40
$SnCl_3$	−2024	2.0	3
Cl	−1004	0.3	3
$(CO)_4(PPh_3)MnCH_2C_6H_4Z$[a] **11b**	−1838 to −1777	0.4–0.6	40
$(CO)_4(PPh_3)MnC(O)CH_2C_6H_4Z$ **12**	−1682 to −1660		40
$(CO)_4(PEtPh_2)MnCl$	−1080		41
13 (R_1 = Me, $R_2 = CO_2Me$, C_6H_4Z)	−807 to ca. −970	18–26	42, 43
14 (R_1 = Me, CH_2Ph; $R_2 = CO_2Me$)	−690 to −670	13–27	42
$(CO)_5MnCH_2$–CH=CH(CO_2Et) **15**	−1929		44

[a] $^1J(^{31}P$–$^{55}Mn)$ coupling constants vary between 208 and 298 Hz.

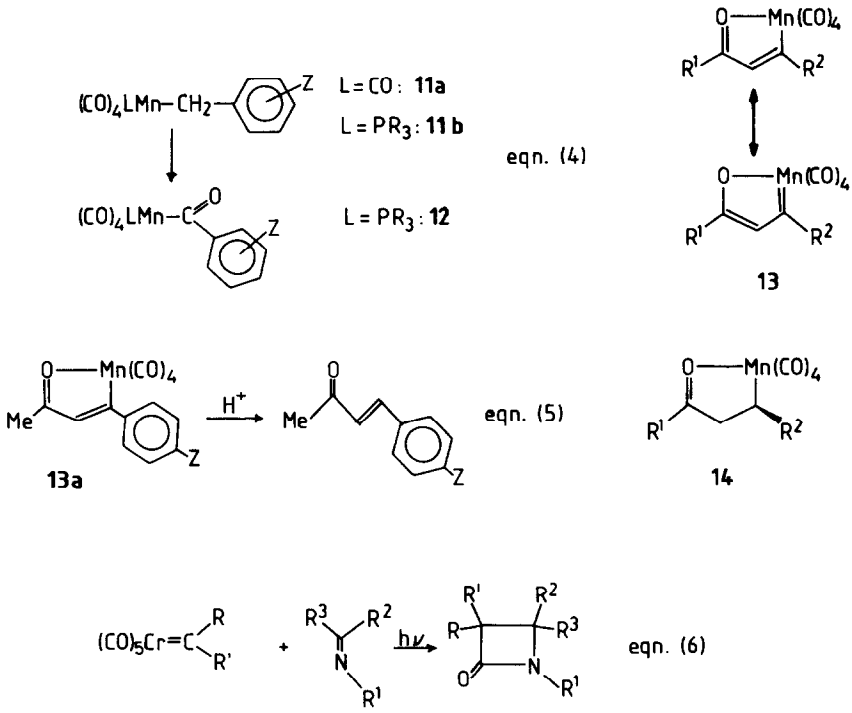

Scheme 2.

has been shown to be formed along with $Mn_2(CO)_{10}$ and $BrMn(CO)_5$ in the reaction between $Na[Mn(CO)_5]$ and 4-bromocrotonic acid ethyl ester [44].

(iv) Groups 8–10

Several direct ^{57}Fe and ^{59}Co measurements on systems relevant to physiological processes have recently been reported. Isotropic $\delta(^{57}Fe)$ values for isocyanide (RNC) myoglobins range from 9223 to 9238 ppm (R = Et, Bu, iPr); the anisotropy values, $|\delta_\perp - \delta_{||}|$, are 1288–1205 [45]. T_1 values (about 140 ms) are much longer than for CO–myoglobin (17 ms; $\delta_{iso} = 8227$ ppm [46]). It has been proposed that it is mainly the shift tensor *perpendicular* to the porphyrin plane that dominates changes in δ_{iso}. ^{59}Co NMR data have been obtained for methylcobalamine ($\delta = 4256$ ppm, $W_{1/2} = 17.3$ kHz) and cyanocobalamin ($\delta = 4750$, $W_{1/2} = 11.1$ kHz) [1].

Information on organometallic compounds with sp^3 and sp^2 carbon is available for most of the iron and platinum metals (for a listing of data up to 1981 see ref. 47). With the exception of ^{59}Co and ^{195}Pt complexes, data are now usually obtained by indirect multidimensional methods, and selected data for compounds carrying a metal–C_σ bond have been included in Table 5. ^{105}Pd and ^{193}Ir have not been used,

TABLE 5

NMR data on alkyl compounds of the iron and platinum metals

Compound	δ(M)[a]	Other data	Method	Ref.
$CpFe(PMe_3)_2R$		^1J(P,Fe) 61	2D(^{31}P,^{57}Fe)	48
$CpFe(PMe_3)_2Me$ **16a**				
$Cp=C_5H_5$	+2342			
C_5H_4Me	+2318			
C_5Me_5	+2679			
$Cp=C_5H_5$				
R = Me	+2342			
Et	+2487			
$CH_2=CH_2$	+2350			
$CpFe\{P(OMe)_3\}_2R$		^1J(P,Fe) 102	2D(^{31}P,^{57}Fe)	48
$R=CH_2CH=CH_2$	+1691			
$CH_2C(Me)=CH_2$	+1744			
$CpOs(PMe_3)_2R$ **16b**			2D(X^b,^{187}Os)	49
$Cp=C_5H_5$, R = Me	−4779	^1J(P,Os) 310		
		^2J(H,Os) 6.4		
Et	−4670	^1J(P,Os) 315		
Ph	−4349	^1J(P,Os) 311		
(COD)Rh{CP} **17**[c]	−8278		2D(^{1}H,^{103}Rh)	50
ClRhH{PCP} **18**[c]	−7339	^1J(P,Rh) −122	Direct ^{103}Rh	51
$[PtMe_6]^{2-}$	+358		Direct ^{195}Pt	52
$(PtMe_3X)_2\{SS\}$ **19**[c]			Direct	54
X = Cl	+1360			
Br	+1266			
I	+1102			
fac-$[PtMe_3(H_2O)_3]^+$	+2543	^1J(C,Pt) 791	Direct	53
20a				
		$^2J(\underline{H}_3C,Pt)$ 80		
		$W_{1/2}$ 48		
fac-$[PtMe_3(CN)_3]^{2-}$	+275		Direct	53
20b				
$[PtMe_2(H_2O)_2OH]^+$	+3950	^1J(C,Pt) 611	Direct	53
21a				
		$^2J(\underline{H}_3C,Pt)$ 76		
$[PtMe_2(H_2O)_2Br]^+$ **21b**	+3135		Direct	53
$PtR_2(PR'_3)_2$				
R = Me **22a**			Direct	55
$2PR_3$ = dppm	+643	^1J(P,Pt) 1427		
		^1J(C,P) 640		
dppe	−70	^1J(P,Pt) 1783		
		^1J(C,Pt) 610		
dppb	−119	^1J(P,Pt) 1847		
		^1J(C,Pt) 600		

TABLE 5 (*Continued*)

Compound	δ(M)[a]	Other data	Method	Ref.
R = Me, $2PR_3 = (Ph_2PCH_2O)_2Zr(Me)Cp^*$ **22b**[c]				57
	−168	^1J(P,Pt) 1830	Direct	
		$^2\Delta^{Pt}(^2H)$[d] −1.3		
R = Me, R′ = Et	−131	δ_{11} −266,	Direct[f]	58
		δ_{22} +127, δ_{33} +536		
R = C≡CH, R′ = *n*Bu **22c**			Direct	56
trans	−251	^1J(P,Pt) 2394		
		^1J(C,Pt) 951		
		^2J(C,Pt) 268		
cis	−273	^1J(P,Pt) 2219		
		^1J(C,Pt) 1080		
		^2J(C,Pt) 302		
23[c,e]	[c]	[c]		15

[a] Cf. Table 1.
[b] ^1H or ^{31}P.
[c] See Scheme 3.
[d] Two-bond isotope shift of the ^{195}Pt resonance per each ^2H, induced by the methyl hydrogens. The negative sign indicates an upfield shift for the heavier isotopomers.
[e] Shift data and coupling constants [J(Pt,Pt) and J(W,Pt)] for many related systems have also been reported.
[f] Solid state measurement; the shielding tensors are for a spinning frequency of 3000 Hz.

owing to their large quadrupole moments (0.8×10^{-28} and 1.4×10^{-28} m^2) and low detection frequencies (4.58 and 1.87 MHz at 2.35 T).

Shielding trends are comparable with what is observed with the transition metal nuclei of Groups 3–7. The deshielding on going from Cp to Cp* (**16a**) and sp^3 to sp^2 carbon (**16**) will be addressed in detail in Sect. E. Replacing a weak acceptor or a ligand not at all capable of delocalizing electron density from the metal centre by a strong π acceptor enhances shielding as a consequence of increased HOMO–LUMO splitting [eqn. (3)]. Examples for this π effect, which counteracts the polarizability effect, are the complexes $CpFe(PR_3)_2R'$ (R = Me and OEt) and the $Pt^{(IV)}$ complexes **20a**/**20b**. Replacement of a hard ligand (OH^-; **21a**) by a soft one (Br^-; **21b**) also increases shielding, which has been traced back to a decrease of the factor $C_{val}\langle r^{-3}\rangle_{val}$ in eqn. (3), Sect. B. (i), for d^n systems. A relativistic "heavy atom effect" [59] adds to the shift through an increase of σ′(dia). This effect is also apparent for the complexes **19**, the polarizability (halogen) dependence of which is normal.

Alkyl complexes of $Pt^{(IV)}$ have been studied extensively (refs. 14 and 53 and the literature cited therein), and only a few selected examples that allow for the presentation of some of the more general shielding trends have been chosen for this review. The ^{195}Pt nucleus is usually less shielded in $Pt^{(IV)}$ than in $Pt^{(II)}$ complexes, although the ranges overlap, underscoring the importance of the paramagnetic term in eqn. (3). In the chelate complexes of the $Pt^{(II)}$ series, **22a**, a "chelate-ring size effect" is

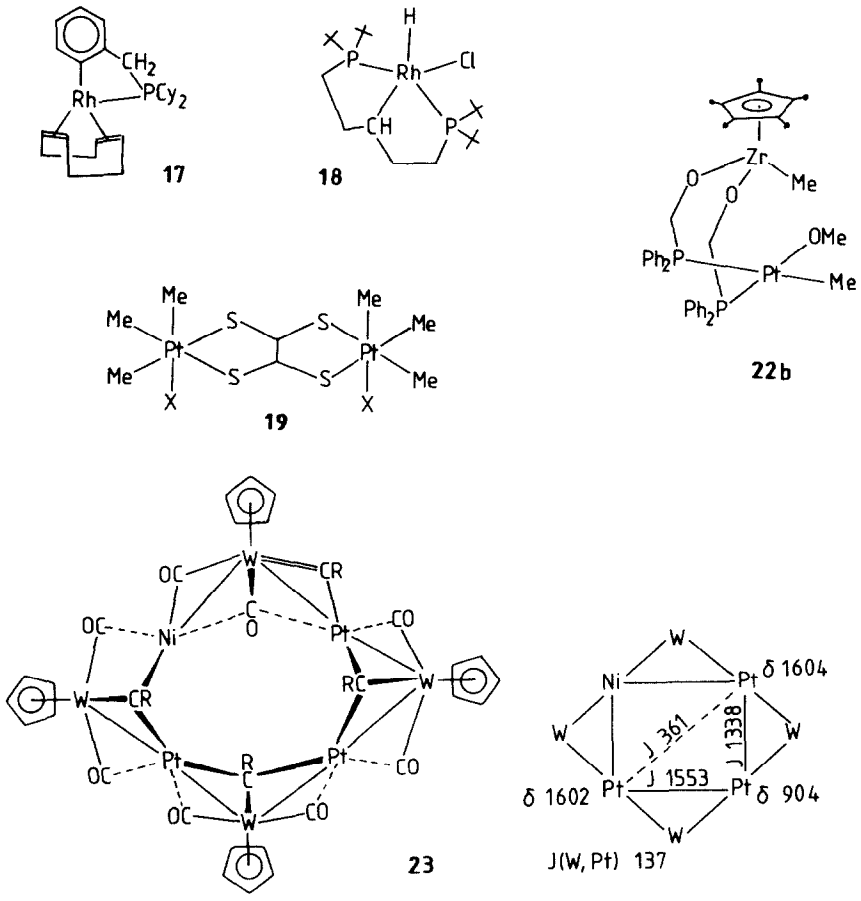

Scheme 3.

observed: The 5-membered ring, which is the least strained one, exhibits a "normal" shielding, while the strained 4-membered ring formed with dppm gives rise to a significant deshielding. The effect can be traced back to P–M–P bonding angles, which largely deviate from the optimum 90° in 4-membered rings (the dppm complex). This leads to non-optimal overlap between bonding orbitals located on P and Pt, and hence to a decrease of ΔE in eqn. (3) and also a decrease of the σ(s) contribution to the coupling interaction, which is one of the dominating parameters in the Fermi contact term of J. Consequently, a comparatively small $^1J(^{31}P-^{195}Pt)$ is observed in the dppm complex. For a more detailed discussion of the chelate effect in metal shielding see, for example, refs. 3 and 60.

Another point worth noting is the effect of geometrical isomerism in metal shielding, which may be expected, since ΔE and C_{val} are composite parameters, averaged over several allowed electronic transitions. Transitions are allowed to

excited levels (LUMOs) which, in a magnetic field, can couple with the ground state (HOMO) via the angular momentum operator, i.e. have the same transformation properties, which again depend on the point symmetry of the compound under consideration. The effect has been treated theoretically by Juranić [8,61]. As an example, in the square-planar $Pt^{(II)}$ complexes **22c**, the ^{195}Pt nucleus is shielded more effectively in the cis than in the trans complex.

A solid state ^{195}Pt NMR study on $Me_2Pt(PEt_3)_2$ [58] has revealed a chemical shift anisotropy of ca. 800 ppm (see Table 5 for the shielding tensor parameters), an order of magnitude typical for Pt in a square planar array, and a main factor contributing to the relatively short spin-lattice relaxation times T_1. Typical T_1 values are in the range of 0.1 to 1 s [12].

A ^{195}Pt crossover experiment of compound **22b** (Scheme 3), utilizing ^2H isotope shifts, has demonstrated that the methyl groups on Zr and Pt exchange. The scrambling as revealed in the ^{195}Pt NMR is illustrated in Fig. 1. The ^{195}Pt resonance upfield isotope shift amounts to 3.8 ppm per CD_3.

(v) Cadmium and mercury. Biological speciation of mercuric compounds

There is abundant data available on organocadmium compounds and organomercurials which have been referenced in, for example, ref. 14. The reader may

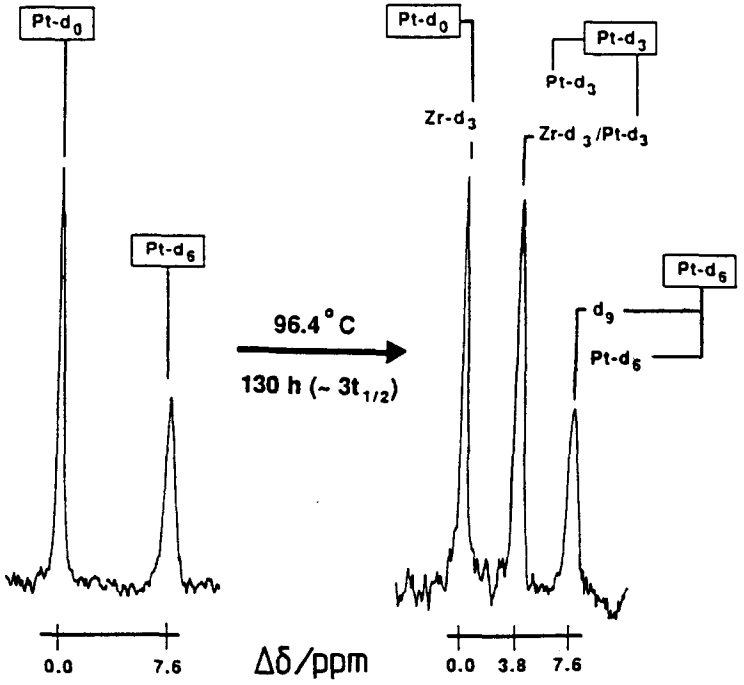

Fig. 1. The $^{195}Pt\{^1H\}$ NMR spectrum of a mixture of **22b**-$Zr(d_3)$,$Pt(d_0)$ and **22b**-$Zr(d_3)$,$Pt(d_6)$ (left) reveals the formation of **22b**-$Pt(d_3)$ isotopomers after heating (right), owing to a scrambling process. (See ref. 57.)

consult refs. 62 and 63 for early and comprehensive reports dealing with ^{113}Cd NMR (nuclear spin $I = 1/2$, natural abundance $N = 12.26\%$) and ^{199}Hg NMR ($I = 1/2$, $N = 16.84\%$) of organo-Cd/Hg. Both nuclei are relatively easily detected, and despite the $I = 1/2$, T_1 relaxation times are reasonably short (e.g. 0.87 s for neat $HgMe_2$ at 27 °C [63]; chemical shift anisotropy is an important factor in relaxing this nucleus) to allow for spectra to be run within a reasonable period of time. Selected data are collated in Table 6.

A theoretical study of cadmium compounds, including $CdMe_2$, has shown that variations in the paramagnetic deshielding term are dominated by variations in $\langle r \rangle_{4p}$ [64] rather than variations in the valence-d imbalance as observed for the transition metals of Groups 3–10. This feature appears to be quite a general one for the group 12 metals and is supposed to explain the increase of shift with increasing electron-donating ability of the ligand. However, as shown by the series MeHgX (X = Cl < Br < I < Ac) and $Hg(ER_3)_2$ [E = Si < Ge < C(alkyl) < C(aryl)], the interrelations are more complex. From a phenomenological point of view, shielding in HgRR' roughly increases with increasing ionic character of the M–R bond. An increase of coordination number may result in an *in*crease or *de*crease of shielding. $HgMe_2$ (and other mercurials) exhibits a notable solvent dependence on the chemical shift (Table 6). Depending on the Lewis basicity of the solvent, the amount of Lewis adduct $Me_2Hg(solv)$ in equilibrium with $HgMe_2$ increases and shifts the ^{199}Hg resonance to higher field. On the other hand, shielding of HgPhCl drastically decreases as triphenyl phosphine is added as a third ligand. Coupling constants $^1J(^{199}Hg–^{13}C)$ are less sensitive to medium effects except where the carbon ligand is highly polarizable, as in alkynyl compounds [75].

Cadmium and mercury are highly toxic, and anthropogenic contamination of our environment with these metals in their elemental state or in the form of inorganic and organic compounds remains a severe problem. Mercury and mercury compounds undergo a variety of chemical and biological speciations within and outside living organisms. NMR spectroscopy can help to identify species or, if natural concentrations are too low for an in vivo detection, to evaluate speciation pathways in model reactions. Equation (7) summarizes some of the compounds arising from the speciation of inorganic HgX_2, with X usually Cl in sea water. Relevant data are contained in Table 6.

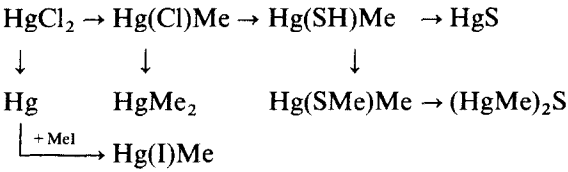

(7)

The non-enzymatic in vitro methylation of $HgCl_2$ by transmethylation with Me_4Pb

TABLE 6

^{113}Cd and ^{199}Hg NMR data

Compound	Medium	δ(M)	Other data	Ref.
$CdMe_2$	Neat			62
$CdPr_3$	Neat	−139		62
$CdPh_2$	1 M dioxan	−314		62
Cd(OR)Me		−295 to −383		65
Cd(SR)Me		−31 to −44		65
$HgMe_2$	1 M dmso	−108.8		63
	1 M toluene	−50.1		63
	1 M hexane	+5.3		63
HgRR′	1 M dmso[a]			63
R, R′ = Et		−364.7		
Ph		−808.5		
C≡CH		−978.3	^1J(Hg–C) 2656	
			^2J(Hg–C) 652	75
SiH_3 (benzene)		+197	^1J(Hg–Si) 981[b]	46
GeH_3 (C_6D_6/C_6F_6)		−147		66
Cl		−1501.6		63
SEt		−985		69
R = Me, R′ = Cl		−847.9		63
Br		−959.1		63
I		−1142.6		63
Ac		−1101.3		67
SPh ($CDCl_3$)		−580.8	$^1J(Hg–C_{Me})$ 1128	70
SMe (CH_2Cl_2)		−497		71
Nucleoside[c]		−620 to −970		68
C≡CH		−555.7	$^1J(Hg–C_{Me})$ 1245	
			$^1J(Hg–C_\alpha)$ 1447	
			$^2J(Hg–C_\beta)$ 409	75
R = Et, R′ = $OP(OEt_2)_2$		−835	^1J(Hg–P) 9266	72
R = Ph, R′ = Cl		−1186.6		63
$PhHgCl(PPh_3)$		−435	^1J(Hg–P) 4610	73
$(MeS)_2Hg$ (CH_2Cl_2)		−316		71
$CH_{4-n}(HgCl)_n$ (dmso)				74
n = 1		−852.3	^2J(Hg–H) 221.4	
2		−758.4	173.3	
3		−677.3	124.5	
4		−622.7		

[a] Unless indicated otherwise.

[b] For $Hg(SiMe_3)_2$, δ = +499 ppm [66].

[c] Cf. Scheme 4.

in sea water has been detected by ^{199}Hg NMR at a concentration level of 2.5×10^{-2} M. A binomial quartet at -873 ppm [$^2J(^1H-^{199}Hg) = 225$ Hz] observed after 12 h of mixing the two components was indicative of complete conversion of $HgCl_2$ to Hg(Cl)Me [76]. The chemical shift of $HgCl_2$ itself depends on pH and on the concentration of Cl^- as a consequence of $[HgCl_3]^-$ and $[HgCl_4]^{2-}$ in equilibrium with $HgCl_2$. Limiting $\delta(^{199}Hg)$ values in aqueous solution are: $HgCl_2 = -1590$, $[HgCl_3]^- = -298$, $[HgCl_4]^{2-} = -1170$ ppm [77]. Replacement of Cl^- in $HgCl_2$ or MeHgCl by a thiolate ligand leads to a shielding decrease, as does the exchange of Cl^- with N donors. Polyfunctional ligands such as nucleosides exhibit a complex coordination pattern [68]. This is shown for selected examples of the coordination of purines to the MeHg moiety in Scheme 4.

C. COMPLEXES CONTAINING π-BONDED ALKENES AND ALKYNES

(i) Groups 4–6

Data are summarized in Table 7. For LZr(η^4-diene), shielding decreases in the sequence L = Cp > allyl > COT. In the series $Cp_2Zr(\eta^4$-diene), there is a decrease in ^{91}Zr shielding in the sequence butadiene > methyl butadiene > dimethyl butadiene, i.e. with increasing steric requirement and/or electron density in the π cloud (sometimes referred to as the "stereo-electronic effect" [1]). The consistently high ^{91}Zr shielding in $Cp_2Zr\eta^4$-diene as compared with $Cp_2ZrL'_2$ (L' = halogen, alkyl) has been explained, based on MO considerations (Fig. 2), in terms of the smaller ΔE [cf. eqn. (3)] for the latter. A substituent effect is also evident for the complexes

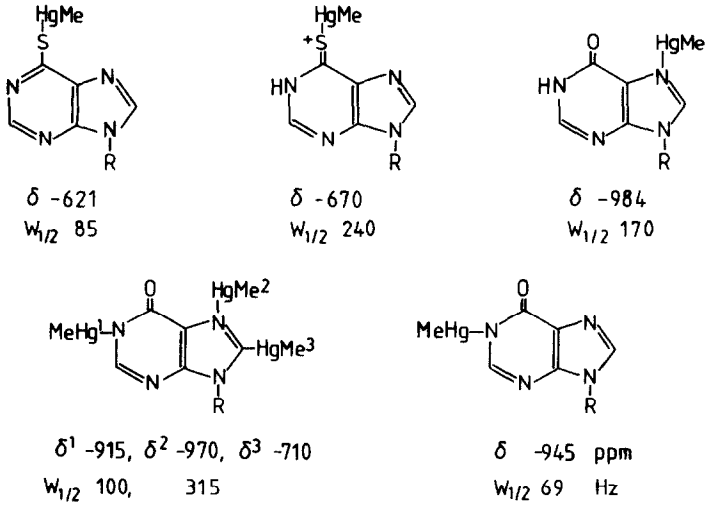

Scheme 4.

TABLE 7

NMR data for π alkene and alkyne complexes

Compound	δ(M)[a]	Other data[a]	Ref.
(η^8-COT)Zr(η^4-butadiene)	+148	$W_{1/2}$ 220	23
CpZr(η^3-allyl)(η^4-butadiene)	+90	$W_{1/2}$ 1.4	23
$Cp_2Zr(\eta^4$-diene)			23
diene = 2,3-dimethylbutadiene	−257	$W_{1/2}$ 1.9	
isoprene	−324	$W_{1/2}$ 2.2	
cis/trans-butadiene	−384	$W_{1/2}$ 3.1	
Cp*V(CO)$_2$(η^2-C_2H_2)	−560		78a
(η^5-Indenyl)V(η^2-C_2H_2)	−455		78a
CpV(CO)$_2$(η^2-C_2RR')			78b
R, R' = H	−598		
Me	−658		
Ph	−626		
$SiMe_3$	−265		
Cp*V(CO)(PMe_3)(η^2-C_2H_2)	−296	J(P,V) 322	78a
$V_2\{\mu$-$(C_5H_4)_2SiMe_2\}(\mu,\eta$-COT) **23**[b]	+1140[c]	$W_{1/2}$ 13.8[c]	79
[V(CO)$_5$(η^2-cyclohexene)[d]	−1772		81
[V(CO)$_5$(η^2-1-hexyne)[d]	−1656		81
Mo(η^4-isoprene)$_3$[e] **24a**[b]	−1717	T_1 0.3	82
24b[b]	−1723	T_1 1.6	82
Mo(η^6-C_7H_8)$_2$	−457	$W_{1/2}$ 150	84
W(η^4-isoprene)$_3$[e] **25a**[b]	−3277	T_1 5.4	82
25b[b]	−3279	T_1 5.5	82

[a] Half-width $W_{1/2}$ (Hz), coupling constant J (Hz), spin lattice relaxation time T_1 (s).
[b] See Scheme 5.
[c] Data are given for 298 K in toluene-d_8. At 200 K: $\delta = +1283$, $W_{1/2} = 1.5$ kHz. Data for the corresponding μ-$GeMe_2$ and μ-CH_2 complexes have also been reported.
[d] 220 K in THF.
[e] 310 K in toluene-d_8.

CpV(CO)$_2$(η^2-C_2R_2) (Table 7) with alkynes donating four electrons. These vanadium complexes exhibit a surprisingly low shielding [compare the parent CpV(CO)$_4$: −1525 ppm], considering the low oxidation state ($V^{(I)}$) and the presence of the effectively π accepting alkyne ligands. The same is true, although not to this extent, for the complexes [V(CO)$_5$L]$^-$ (with L a two-electron-donating alkene or alkyne) derived from [V(CO)$_6$]$^-$ ($\delta = -1952$ ppm).

The dinuclear complex **23** (Scheme 5) formally contains a vanadium–vanadium triple bond ($\sigma^2\pi^2\delta^2$) [79]. The extreme deshielding of the ^{51}V nuclei is very reminiscent of the situation found in triply bonded Mo and W complexes (see the preceeding section). The extreme temperature gradients of $\delta(^{51}V)$ ($\Delta\delta$ is 143 ppm for the resonance

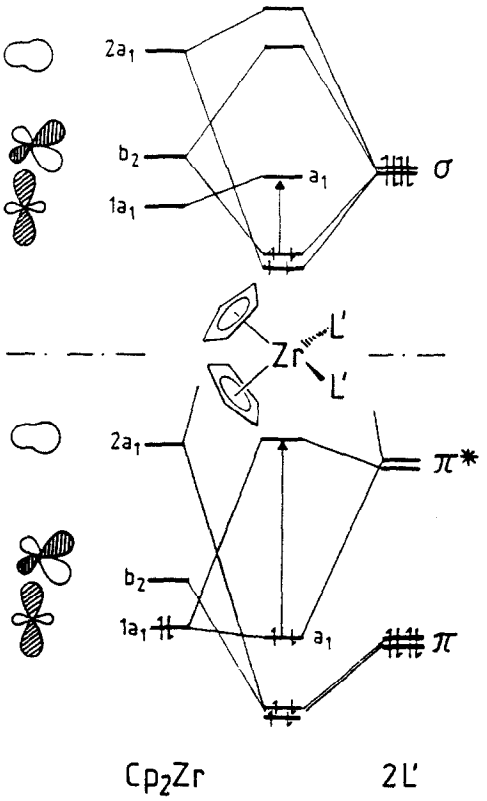

Fig. 2. Qualitative MO diagrams for $Cp_2ZrL'_2$ for L' = halogen or alkyl (above) and L'_2 = olefin (HOMO–LUMO gap = 2.3 eV for olefin = butadiene). Redrawn from ref. 2.

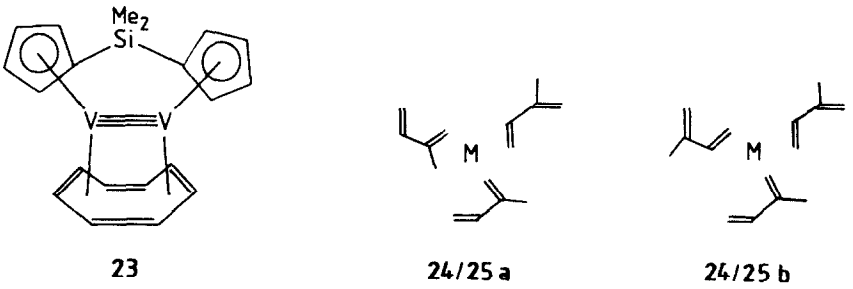

23 24/25 a 24/25 b

Scheme 5.

positions at 200 and 298 K, respectively) and $W_{1/2}(^{51}V)$ reflect the temperature dependence of antiferromagnetic coupling between the two vanadium centres. Temperature gradients normally observed for low-valent vanadium complexes range between ca. 0.3 and 1 ppm deg^{-1} [80].

(ii) Groups 8–10

^{57}Fe MNR data for organoiron complexes containing various ligands including dienes have been reviewed by von Philipsborn [1] and ^{57}Fe chemical shifts are depicted schematically, in relation to other coordination compounds of iron, in Scheme 6 (from ref. 1). Table 8 contains selected data, including more recent data for iron and osmium olefin complexes obtained by indirect methods (mainly indirect 2D hetreonuclear spectroscopy).

All organoiron compounds exhibit a consistently higher shielding of the ^{57}Fe nucleus than coordination complexes carrying classical ligands, including cyanide. The shift scale is limited on the high-field side by the half sandwich $(CO)_3Fe(\eta^4$-cyclo-$C_4H_4)$ (−583 ppm) and by $Fe(CO)_5$ (0 ppm). There is a decrease in shielding as CO in $Fe(CO)_5$ is gradually replaced by π bonding ligands [$Fe(CO)_5$ > {$Fe(CO)_3$} (**26**) > {Fe(CO)} (**27**)], in accord with what has been noted in the previous section. In the Fe(diene) complexes **26**, there is a substituent effect comparable with what has been described for Zr(diene) compounds.

Spin-lattice relaxation times, T_1, for the diene complexes (Table 8) are much longer than in ferrocenes (around 1 s) [1].

The shielding situation encountered in Fe(diene) complexes is also similar to that observed in Co(diene) and Rh(diene) complexes (Table 9 and, for Rh compounds, Scheme 7), in that shielding of the metal nuclei is consistently high, approaching that of the simple binary carbonyl species. There is again an influence of diene geometry

TABLE 8

NMR data of iron and osmium compounds containing olefin ligands

Compound	δ(M)	Other data	Ref.
$(CO)_3Fe(\eta^4$-diene) **26**			1, 83
diene = cyclo-1,3-hexadiene	−72.9		
butadienes RCH=CH–CHR′			
R, R′ = H	+16.9	T_1 23[b]	
R = H, R′ = Me	+31.7	T_1 19[b]	
R, R′ = Me	+86.4		
R = Me, R′ = CO_2Et	+312.3		
$(CO)_3Fe(\eta^4$-cycloheptatriene)	+170		1
$(CO)Fe(PP)(\eta^4$-1,4-cyclo-$C_6H_8)$[a] **27**	+2040	J(P,Fe) 49	38
$Cp^*Fe(H)(PMe_3)(\eta^2$-$C_2H_2)$ **28**	+1480	J(P,Fe) 55	48
$Cp^*Os(H)(\eta^4$-COD)	−4889	T_1 5.6(6)	85
$CpOs(R)L_2$			49
R = η^2-C_2H_4, L_2 = $2PPh_3$	−4401	J(P,Os) 266	
R = H, L_2 = η^4-1,5-COD	−4889	J(H,Os) 64.3	

[a] PP = $iPr_2PCH_2CH_2PiPr_2$.

[b] At 9.4 T. T_1 values at 2.1 T are 84 (butadiene) and 88 s (isoprene), respectively.

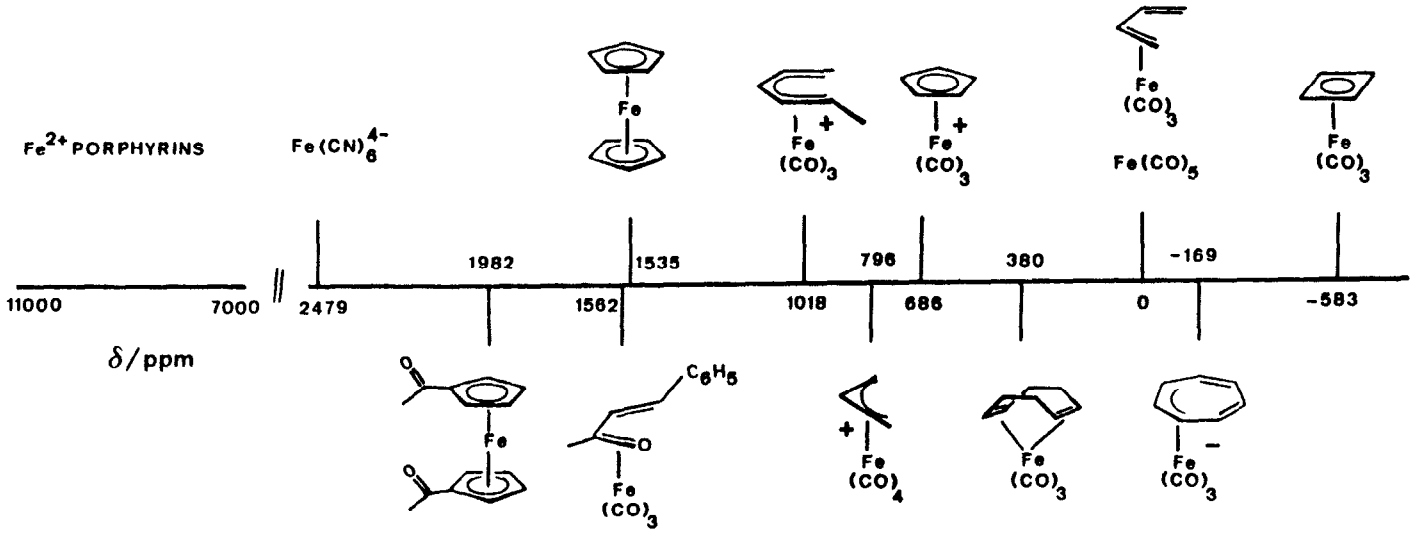
Fe2+ PORPHYRINS
Fe(CN)6 4-
11000
7000
δ/ppm
2479
1982
1562
1535
1018
796
686
380
0
-169
-583
Fe
Fe(CO)3
Fe(CO)5
Fe(CO)4
C6H5
O

Scheme 6.

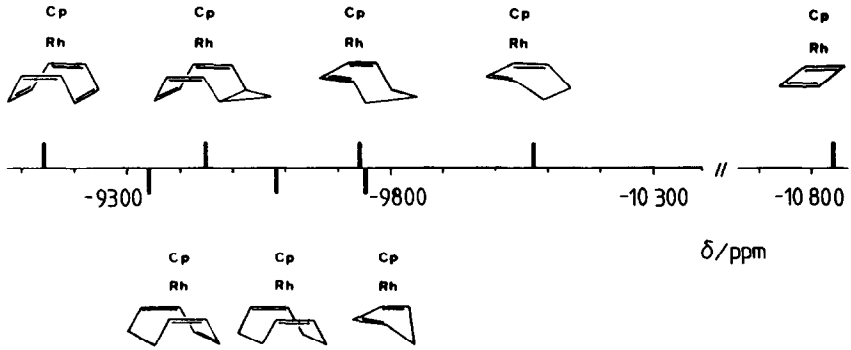

Scheme 7.

and substitutents on the diene backbone. For the cobalt complexes CpCo(diene), there is a striking dependence of $\delta(^{59}Co)$ on the ring size, i.e. generally an increase in shielding as bond angles increase (see the ordering for the class **27** compounds in Table 9; cyclobutadiene has been included).

The substituent pattern is rather complex (see, for example, **27a** and **27b** in Table 9). For diene = substituted butadiene, von Philipsborn [1] has noted the shielding influences on methyl substitution depicted for **28** in Scheme 8.

Several papers address the relationship between ^{59}Co shielding and the catalytic activity of LCo(diene) complexes (L = allyl, Cp and indenyl) in pyridine formation from olefins and nitriles [2,86]. Activity variations are mainly an outcome of effects imparted by substituents on the L ligand and will be dealt with in detail in section E.(v). Note, however, that compounds which cannot be thermally activated [LCo(diene) → LCo + diene] at moderate temperatures, such as CpCo(cyclobutadiene) with an extremely shielded ^{59}Co nucleus, are inactive [86(a)].

^{103}Rh NMR patterns are similar to those in iron and cobalt complexes. An extensive listing is found in refs. 17 and 18. Selected examples are contained in Table 9 and presented schematically in Scheme 7 (from ref. 18). Apart from the influence of diene geometry on $\delta(^{103}Rh)$ depicted in Scheme 7, there is also an effect on the coupling constants $^1J(^{13}C\text{-}^{103}Rh)$. As noted in Table 9 for CpRh(1,3-diene), increasing ring-size of the carbocycle leads to an increase of coupling interaction with outer carbons, and to a decrease with the inner carbons of the double bonds.

The usefulness of direct ^{103}Rh NMR as an analytical tool has been demonstrated in several cases. Thus, the dinuclear complexes **30** (cf. Scheme 8) give rise to two ^{103}Rh NMR signals for the $CpRh^I$ unit, and the Rh^0(nor) and $Rh^0(CO)_2$ moieties, respectively. The signals to higher field have been assigned to $Rh^{(I)}$ [18]; the large shift differences have been attributed to the two distinct oxidation states of Rh. Large shift differences, although not to this extent, may also arise, as shown for compounds **31**, from differing coordination environments. In **31**, the two CpRh groups are non-

TABLE 9

NMR data for cobalt, rhodium and platinum compounds containing olefin ligands

Compound	δ(M)	Other data[a]	Ref.
CpCo(diene) **27**			
diene = cyclobutadiene[b]	−2888		86(a)
1,3-cyclo-C_6H_4(1,2,3,4-R_4)			87
R = H	−1820	$W_{1/2}$ 13.0	
CF_3 **27a**	−1726	$W_{1/2}$ 14.4	
Ph **27b**	−930	$W_{1/2}$ 18.8	
butadiene	−1620	$W_{1/2}$ 8.7	87
cyclopentadiene	−1439	$W_{1/2}$ 9.6	87
1,3-cycloheptatriene	−1400	$W_{1/2}$ 10.1	87
2 ethene	−1235	$W_{1/2}$ 6.8	87
1,4-COD	−602	$W_{1/2}$ 9.2	86(a)
IndCo(butadiene) **28**	−1234	$W_{1/2}$ 11.2	87
$[(1,4\text{-COD})RhH]_4$	−7520	^1J(H,Rh) 14.3	38
(acac)Rh(diene) **29**[c]	−6918	J(H,Rh) 1.2–2.1	38
(acac)Rh(ethene)$_2$	−7126		2
(acac)Rh(1,4-COD)	−7014		2
$[ClRh(1,4\text{-COD})]_2$	−7205		2
(COD)RhL_2			17
2 L = acac	−7014	J(C,Rh) 14	
Cl + pyr	−7271		
bipy	−7493	J(C,Rh) 13	
Cl + PPh_3	−7913	J(C,Rh) 14/12	
		J(P,Rh) 149	
$CpRh(PPh_3)$(ethene)	−9330	J(P,Rh) 208	50
CpRh(diene)[d]			1, 18
diene = cyclobutadiene[e]	−10 831	J(C,Rh) 11.7	
cyclopentadiene	−9732	J(C,Rh) 11.9/9.4	
1,3-cyclohexadiene	−10 046	J(C,Rh) 15.4/7.3	
1,3-cyclooctadiene	−9559	J(C,Rh) 17.4/6.1	
		T_1 60, T_2 27	
$[CpRh(\mu\text{-COT})Rhnor]^+$ **30a**	−10 576/−8857		18
$[CpRh(\mu\text{-COT})Rh(CO)_2]^+$ **30b**	−10 431/−9484		18
$(CpRh)_2(\mu\text{-}C_7H_8)$ **31a**[e]	−9916/−9450		18
$(CpRh)_2(\mu\text{-}C_8H_8)$ **31b**[e]	−9854/−9508		1
$Pt(1,4\text{-COD})_2$	−103	T_1 0.15[e]	88
$(Ph_3P)_2$Pt(cyclopropene)	−580	T_1 0.25[e]	
		J(P,Pt) 3393	88
(dtpe)Pt(η^2-butadiene)[f]	−717	T_1 0.17[e]	88
		^1J(P,Pt) 3248/3227	
$Pt(styrene)_3$[h] (263 K)	−1382/−1364		90
$[PtCl_3(styrene)]^-$	+1950		89
trans-$[PtCl_2(styrene)_2]$ *trans*-**32**	+1913		90
cis-$[PtCl_2(styrene)_2]$ *cis*-**32**[g]	+1353/+1232/+1212		89
trans-$[PtCl_2(styrene)NH_2Ph]$	+1691	$J(^{15}N,Pt)$ 244	90

TABLE 9 (*Continued*)

Compound	δ(M)	Other data[a]	Ref.
cis-[$PtCl_2$(styrene)NCPh]	+1813		90
trans-[$PtCl_2$(ethene)imin][i] (*E*)	+1810		92
(*Z*)	+1660	*J*(C,Pt) 210	
trans-[$PtCl_2(\eta^2$-allen)NH_2CH(Me)Ph **34**[j]	+1921/+1916/+1933/+1937		93

[a] $W_{1/2}$ in kHz, *J* in Hz, T_1 and T_2 in s.
[b] See also section E. (π-arene complexes.)
[c] See Scheme 8.
[d] The first value for the *J*(C,Rh) is the coupling to the *exo*, the second to the *endo* carbons of the double bonds.
[e] At 9.4 T.
[f] dtpe = $(t$Bu$)_2PCH_2CH_2P(t$Bu$)_2$.
[g] In CD_2Cl_2 at 183 K; three isomers; see also text and Scheme 9.
[h] In toluene-d_8/styrene 1/10; two isomers.
[i] Imin = *N*-methyl-1-(*N*-methylpyrrol-1-yl)ethaneimine, coordinating through the imine-N. A variety of other species belonging to this class of complexes has also been reported.
[j] Four diastereomers; see text, Scheme 9 and Fig. 3.

equivalent despite their fluxional behaviour, in accord with one of the CpRh groups always bound in the $\eta^3(\sigma, \pi)$, the other one in the $\eta^3(\pi$-allyl) mode [1,18].

^{195}Pt NMR investigations on platinum complexes containing olefinic ligands have recently been employed to tackle problems such as isomerism and species formed in catalytic turnover, where ^{1}H and ^{13}C NMR spectroscopy did not provide a satisfying answer. As an example, ^{195}Pt investigations into the catalysis [using $PtCl_2$(styrene)$_2$, **32**, as the catalyst] of hydrosilylation by Et_3SiH of styrene have revealed that the primary product formed is *trans*-**32**, which converts to the active precursor *cis*-**32**. The hydrosilylation itself proceeds via reduction of *cis*-**32** to the Pt^0 complex Pt(styrene)$_3$ [90]. In solution, *cis*-**32** exists in the form of three isomers, *cis*-**32a**, *cis*-**32b** and *cis*-**32c** (Scheme 9) with distinctly different $\delta(^{195}Pt)$ values (Table 9). The isomer initially present as solid *cis*-**32** is dissolved in CD_2Cl_2 at 183 K is *cis*-**32b**, the main component after isomerization is *cis*-**32c** [89]. The catalysis of the reduction by silanes of organic carbonyls by *cis*-**32** needs a co-catalyst, viz. aniline, and it has been shown, again by ^{195}Pt NMR, that *trans*-[$PtCl_2$(styrene)NH_2Ph] is formed as an intermediate [90].

Coordination of prochiral olefins to Pt induces the formation of a pair of enantiomers. In compound **33** (Scheme 9) there are two additional centres of chirality. Of the four possible diastereomers, three have been detected by ^{195}Pt resonances, spanning a range of 50 ppm [91]. This example, among others, clearly demonstrates that steric effects may be responsible for variations in shielding. This is also apparent for the complexes *trans*-[$PtCl_2(\eta^2$-allene)(amine)], **34**, containing a trisubstituted,

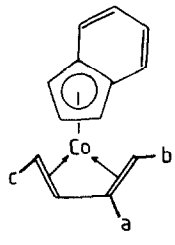

28

	Shielding relative to $IndCo(\eta^4\text{-}C_4H_6)$
a	-15 to -40
b	-20 to -50
c	+15 to +60

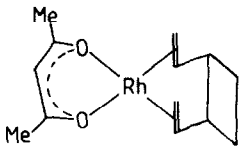

29

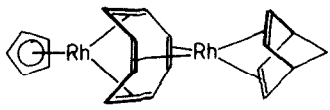

30a

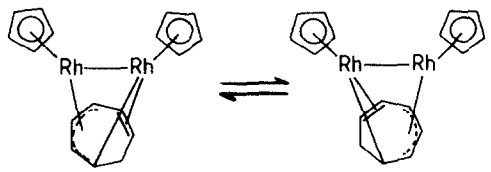

31a

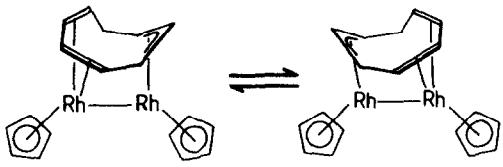

31b

Scheme 8.

chiral allene and an amine with a centre of chirality, α-methyl-benzylamine: four species can be detected in solution (Fig. 3), which are the four diastereomers (two of which are shown in Scheme 9) arising from the coordination to Pt of the two prochiral faces of the sterically less hindered double bond of the enantiomeric allenes [93].

D. η^2-ACYL AND η^3-ALLYL COMPLEXES

These are treated together here, considering the fact that both, the side-on coordinated acyl and allyl ligands, can be considered as three-electron donors. The number of data available on η^2-acyl complexes is restricted, the only systematic

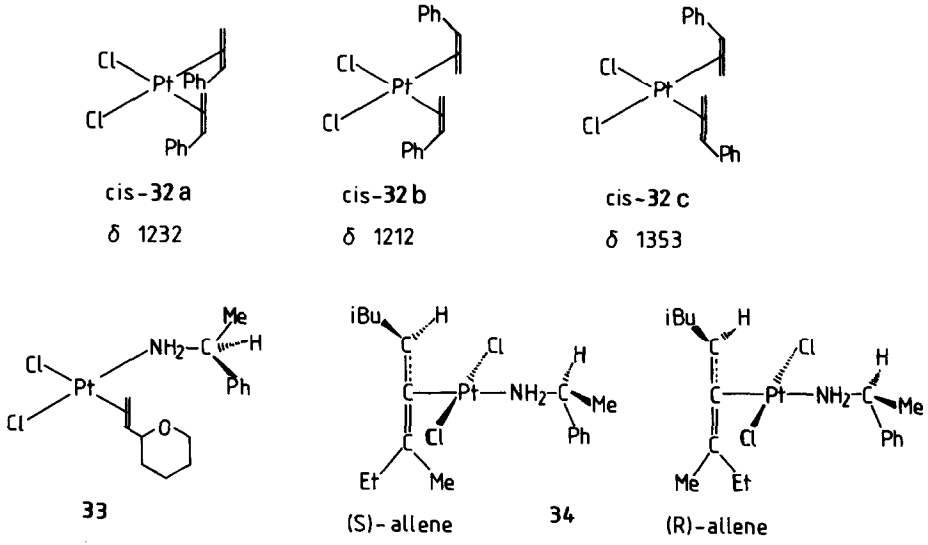

Scheme 9.

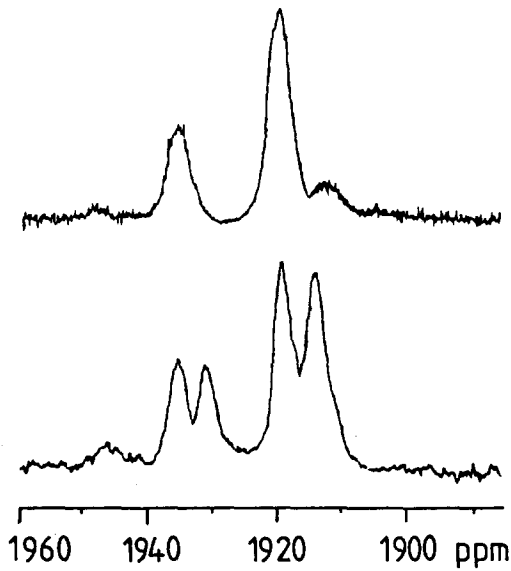

Fig. 3. 64.3 MHz ^{195}Pt NMR spectra of **34**. The upper trace is the spectrum of the complex containing racemic allene. The lower trace corresponds to the situation after enantiomeric enrichment in the *R*-antipode.

investigation being a ^{51}V NMR study on (η^2-acyl)V(CO$_3$)(LL). For data, see Tables 10 (Groups 4–7) and 11 (Groups 8–10).

In allyl complexes, the metal nucleus may be shielded or deshielded with respect to corresponding complexes carrying Cp instead of the allyl ligand. A deshielding effect is apparent in, for example, CpZr{Cp/allyl}diene and has been traced back to the electron deficiency of allyl complexes (16 e) when compared with the Cp analogues (18 e) [23]. On the other hand, where 18-e species are compared, the metal nuclei tend to be more effectively shielded in allyl than in Cp, σ alkyl, η^1-acyl and η^2-acyl complexes. Quite interestingly, the three-electron donor NO in (NO)V(CO)$_3$LL [96] induces a ^{51}V shielding very similar to that observed in (allyl)V(CO)$_3$LL.

Also evident are various effects within a series of allyl complexes (cf. Tables 10 and 11) arising from substituents on the allyl ligand and from the ancillary ligand system. Geminal methyl substituents on the allyl ligand induce deshielding, becoming increasingly effective with increasing methyl substitution. The effect is analogous to that observed in methyl-substituted butadiene complexes. Substitution on C2 may result in additional shielding. The effects imparted by the ancillary ligand system are substantially the same as in other types of complex: (i) a decrease of shielding in Zr(isoprene) compared with the Zr(butadiene), (ii) a decrease on going from chelate-5 to chelate-6 rings in the vanadium compounds carrying bis(phosphines), (iii) a decrease in the molybdenum complexes as CO is exchanged for NO and further for I, and (iv) the normal halogen dependence for (allyl)Fe(CO)$_3$X. In (allyl)Fe(Cp)(PR$_3$), shielding and $^1J(^{31}P-^{57}Fe)$ depend on the nature of R. For R = F (**41**) coupling and ^{57}Fe shielding are largest. A substituent effect has been noted in the complexes {η^2-C(O)C$_6$H$_4$Z}V(CO)$_3$dppe (**35b**): $\delta(^{51}V)$ correlate with the Hammett σ constants of the substituents Z on the phenyl ring [94].

The ^{95}Mo NMR spectra of Mo(allyl) complexes **37** have turned out to be a valuable tool in distinguishing between the *endo* and *exo* coordination of the allyl ligand (Scheme 10), with the *endo* form deshielded by ca. 150 ppm with respect to the *exo* form [95].

Many of the data contained in Table 11 have been obtained by indirect methods, the resolving power of which is greater in many cases than that of direct methods, not counting the considerable increase in sensitivity. The indirect 2D (^{31}P,^{57}Fe) spectrum of (η^3-C$_3$H$_5$Fe(Cp)PF$_3$, **41**), for example, allows for the detection of $^2J(^{19}F-$

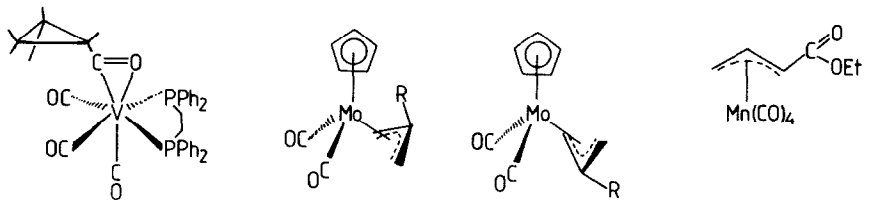

35 36

Scheme 10.

TABLE 10

Data for acyl and allyl complexes of the metals of Groups 4–7

Compound	δ(M)	Other data[a]	Ref.
$C_3H_3Ti(NEt_3)_3/CHCl_3$	−207	$W_{1/2}$ 300	22
$Cp(C_3H_5)Zr$(butadiene)/tol	+90	$W_{1/2}$ 1400	23
$Cp(C_3H_5)Zr$(isoprene)/tol	+123	$W_{1/2}$ 1400	23
$Cp(C_3H_4Me)Zr$(butadiene)/tol	+142	$W_{1/2}$ 2500	23
$Cp(C_3H_3Me_2)Zr$(isoprene)/tol	+268	$W_{1/2}$ 1000	23
$C_3H_5V(CO)_3L_2$/THF,MeCN			3
L_2 = dppe	−1492		
dppp	−1348		
diars	−1461		
{η^2-C(O)R}$V(CO)_3L_2$/THF **35**[b]			94
R = cyclopropyl, L_2 = dppe	−1038	J(P,V) 184	
dppp	−931	J(P,V) 176	
R = C_6H_4Z, L_2 = dppe **35b**		$W_{1/2}$ 480–710	
Z = 4-Cl	−1009		
4-F	−1027		
H	−1027		
4-Me	−1037		
3-OMe	−1022	J(P,V) 169	
2-OMe	−1031		
4-OMe	−1052		
4-NMe_2	−1082		
L_2 = dppe, Z = 4-OMe	−950	$W_{1/2}$ 416	
L_2 = diars, Z = 4-OMe	−1032	$W_{1/2}$ 229	
$Cp(C_3H_5)Mo(L^1)(L^2)$/acetone **37**			95
$L^1 = L^2$ = CO (*endo*, *exo*)	−1658, −1832		
L^1 = CO, L^2 = NO (*endo*, *exo*)	−1530, −1576		
L^1 = NO, L^2 = I (*endo*)	−1093		
$Cp(C_3H_{5-n}X_n)Mo(CO)_2$/acetone			95
n = 0	−1658, −1832[c]		
n = 1, X = 1-Me	−1600, −1789[c]		
2-Me	−1573, −1752[c]		
cyclohexenyl *exo*	−1824		
2-Cl	−1521, −1709[c]		
n = 3, X_3 = 1,1,2-Me_3	−1448, −1657[c]		
$(C_3H_5)_4Mo$/tol, 310 K	−1405	$W_{1/2}$ 17	82
$(C_3H_5)_4W$/tol, 310 K	−3186	T_1 9.7[d]	82
$(C_3H_4R)Mn(CO)_4$/THF, R = H	−2275	$W_{1/2}$ 1600	44
CO_2Et **36**	−1981	$W_{1/2}$ 3000	
CO_2Ph	−1941	$W_{1/2}$ 3100	

[a] $W_{1/2}$ in Hz; J in Hz.

[b] Cf. Scheme 10.

[c] The first value corresponds to the *endo*, the second to the *exo* form (cf. Scheme 10).

[d] T_1 in s at 9.4 T and 310 K. At 273 K, T_1 = 6.6 s.

TABLE 11

η^3-Allyl complexes for the metals of Groups 8–10

Compound	δ(M)	Other data[a]	Ref.
$[(C_3H_{5-n}Me_n)Fe(CO)_4]^+$; $n=0$	+796		1
2[b]	+896		
4[b]	+998		
$C_3H_5Fe(CO)_3X$; X=Cl	+1708		1
Br	+1528		
I[c] **38**	+1235; 1356		
$[(\eta^3\text{-}C_7H_7)Fe(CO)_3]^-$ **39**[d]	−172		1
$(CO)_3Fe\mu\text{-}(\eta^3{:}\eta^4\text{-}C_7H_7)Rh(nor)$ **40**	−223		1
exo-$[C_3H_5Fe(Cp)PR_3]$; R=F **41**	+997	J(P,Fe) 147	48
OMe	+1667	J(P,Fe) 108	
exo-$[C_3H_5Fe(Cp^*)PMe_3]$	+2246	J(P,Fe) 70	48
$(C_3H_5)_3Co$/THF, 245 K	−796	$W_{1/2}$ 3800	87
$(2\text{-}MeC_3H_4)_3Co$/THF, 245 K	−1306	$W_{1/2}$ 13 000	87
$(C_3H_5)Co(Cp)Br$/THF, 245 K	+1050	$W_{1/2}$ 10 000	87
$(C_3H_5)Co(Cp)Me$/THF, 245 K	−788	$W_{1/2}$ 11 000	87
$(CpRh)_2(\eta\text{-}C_7H_8)$/THF **31a**[d]	−9450/−8984		18
$(CpRh)_2(\eta\text{-}C_8H_8)$ **31b**[d]	−9388/−9042		1
$C_3H_5Rh(PPh_3)_2$/THF	−9312	J(P,Rh) 201	50
Pt(allyl)$_2$ *trans*/*cis*	−1670/	T_1 0.40/0.33	88
	−1441	^1J(C,Pt) 3284/3227	
		^3J(C,Pt) 69	
[(2-Me-allyl)Pt$(SnCl_3)_3]^{2-}$ **42**[e]	−318		97
		$J(^{117}Sn,Pt)$ 11 609	
		$J(^{119}Sn,Pt)$ 12 135	
(2-Me-allyl)Pt$(SnCl_3)\eta^2$-styrene **43**[e]	−1353, −1248		98

[a] $W_{1/2}$ in Hz; J in Hz.
[b] The methyl groups are in *geminal* positions.
[c] Two isomers; cf. Scheme 11.
[d] See Scheme 8 and discussion in Sect. C. (ii).
[e] See Scheme 11 and text.

^{57}Fe) coupling (about 3 Hz), which is not resolved in the direct 1D ^{57}Fe NMR [48]. An interesting case to note is the similarity of the $\delta(^{57}Fe)$ value of the C_7H_7 complexes **39** and **40**, indicating that, as the Rh(nor) moiety is coordinated to the anion **39**, only minor charge transfer occurs between the 18 e iron and the 16 e rhodium fragments.

The Pt dianion **42** has been identified, by direct ^{195}Pt NMR [97], as an intermediate in dissociative interconversion between the two isomers of the neutral compound **43** (Scheme 11), which has been characterized by (^{195}Pt,^{1}H)-INVERSE, J-resolved COSY-90 and NOESY methods [97,98].

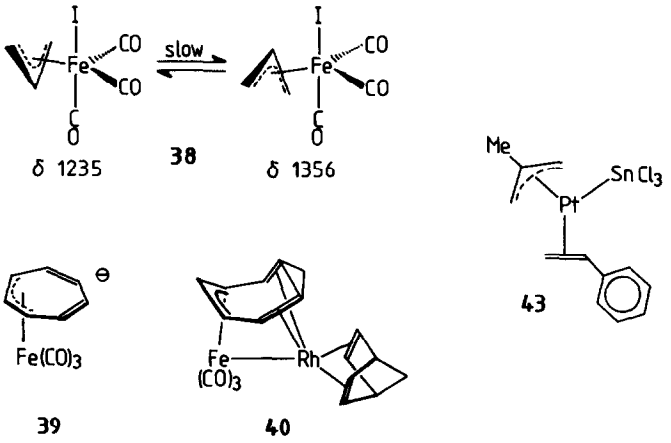

Scheme 11.

E. π-ARENE COMPLEXES

In this section, metal shielding and its dependence on the nature of the aromatic, "sandwiching" ligand will be compared. Since most data were obtained for cyclopentadienyl complexes, effects conveyed by substituted η^5-$C_5H_5^-$ will be emphasized. Shielding variations based on electronic and steric effects in the supporting ligand system, which are usually the same qualitatively as in, for example, η^2-diene or η^3-allyl complexes, will not be discussed here again except where there are synergetic interactions with Cp. In this context, Table 13 (see below) and Fig. 4 (see below) may be consulted for information on the general trends in Cp-V^V and -V^I complexes, which are representative of other closed and open shell systems, respectively. Many of the general aspects concerning half-sandwich complexes will, in fact, be discussed in subsection (ii), since a comprehensive body of data is available on vanadium both in its highest and lowest oxidation state(s). Substituent effects, and the η^5/η^6-$C_5H_4CR_2$ (cyclopentadienyl/fulvene) synergism have also been investigated to some extent in ferrocene derivatives (subsection (iv)). Reactivity patterns related to metal shielding are the subject of the cobalt section (subsection (v)).

(i) Groups 3 and 4

Data are collated in Table 12. The only solution NMR report that has so far appeared on a lanthanide, viz. $^{171}Yb^{(II)}$ [101], is included here. ^{171}Yb is a spin 1/2 nucleus with a natural abundance of 14.27%. Its relative receptivity is four times that of ^{13}C. The ratio $\nu(^{171}Yb)/\nu(^1H(TMS))$ for $Cp^*_2Yb(thf)_2$ in THF-d_8 at 296 K (the standard employed) is 0.175, $T_1 = 1.3$ s at 263 K. The large (and inverse) temperature dependence of $\delta(^{171}Yb)$ of $Cp^*_2Yb(thf)_2$ (+0.69 ppm deg^{-1}) reflects some kind of relatively rapid chemical exchange equilibria, the positions of which are subject

TABLE 12

Cyclopentadienyl complexes of group 3 and 4 metals

Compound	δ(M)	Other data	Ref.
Cp_2ScCl	−10	$W_{1/2}$ 85	99
Cp_2Sc (σ-C_5H_5) **44a**[a]	+14	$W_{1/2}$ 85	99
$\{Cp_2Sc\}_2(\mu$-$C_5H_5)_2$ **44b**[a]	+54		99
Cp_2ScBH_4	+68	$W_{1/2}$ 250	99
$Cp'_3Y(thf)$	−371		19
$Cp'_2YCl(thf)$	−103		19
$\{Cp'_2Y\mu$-X$\}_2$, X=Cl	−97		19
H	−92	J(H,Y) 27	19
Me	−15		19
$\{Cp_2Y\mu$-H$\}_3(\mu_3$-H) **45**[a]	−15		19
Cp'_3La	−380	$W_{1/2}$ 11 100	20
$Cp_3LaNCMe$	−578	$W_{1/2}$ 1200	100
$Cp_3La(NCMe)_2$	−606	$W_{1/2}$ 600	100
$[Cp_3LaX]^-$, X=Cp	−772/−489	$W_{1/2}$ 3070/250	20
BH_4	−550/−474	$W_{1/2}$ 300/550	20
F	−481/−446	$W_{1/2}$ 200/300	20
I	−430	$W_{1/2}$ 1900	20
$Cp^*_2Yb(OEt)_2/Et_2O$ 308 K	+36	$W_{1/2}$ 90; $\partial\delta/\partial T$ +0.25[b]	101
$Cp^*_2Yb(pyr)_2$/pyr 338 K	+949	$W_{1/2}$ 70; $\partial\delta/\partial T$ +1.46[b]	101
$[CpTi(CO)_4]^-$	−1269	$W_{1/2}$ 93	102
Cp_2TiCl_2	−772	$W_{1/2}$ 30	103
$Cp'(Cp)TiCl_2$	−745	$W_{1/2}$ 60	104
$C_5H_4tBu(Cp)TiCl_2$	−782	$W_{1/2}$ 230	104
$Cp^*_2TiCl_2$	−443	$W_{1/2}$ 40	104
Cp_3TiCl	−394	$W_{1/2}$ 36	104
Cp_2ZrCl_2	−113	$W_{1/2}$ 250	23
$Cp^*_2ZrCl_2$	+82	$W_{1/2}$ 90	23

[a] See Scheme 12.

[b] Temperature gradient of $\delta(^{171}Yb)$.

to concentration and medium effects and render this compound a standard of questionable value.

It has been shown by variable-temperature ^{45}Sc NMR that Cp_3Sc (**44a**) in toluene solution is in equilibrium with a dimer, where two Cp_2Sc moieties are bridged by two $\sigma,\pi(C_5H_5)$ (three-electron donating; see **44b** in Scheme 12 for a tentative formulation). In the low-temperature region, monomer and dimer are represented by distinct signals [99]. In the coordinating solvent THF, only a single resonance is observed over the whole temperature range.

Cyclopentadienyl lanthanum complexes cover the range of −380 (Cp'_3La) to −772 ppm ($[Cp_4La]^-$) [20,100]. Coordination of neutral ligands L to Cp_3La such

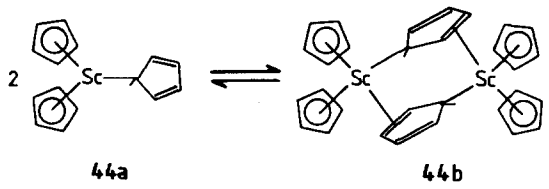

44a 44b

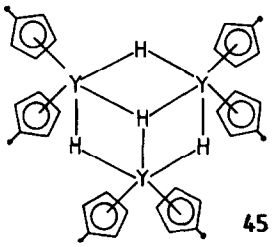

45

Scheme 12.

as amines, nitriles and ethers cause an increase in shielding relative to the parent compound by ca. 130–200 ppm (Cp_3LaL) and ca. 210 ppm (Cp_3LaL_2). $\delta(^{139}La)$ and $W_{1/2}(^{139}La)$ (100–2700 Hz) largely depend on c(L), indicating involvement of relatively rapid exchange equilibria between Cp_3La, Cp_3LaL and Cp_3LaL_2. With negatively charged ligands X^-, Cp_3La forms anionic lanthanates $[Cp_3LaX]^-$ (shift range -430 for X=I to -772 for X=Cp); cf. also the exchange equilibria eqns. (1) and (2) in Sect. B.(i).

(ii) Vanadium

General trends induced by the ancillary, inorganic ligand systems may be extracted, for $V^{(V)}$ complexes, from the data given in Table 13, and, for the $V^{(I)}$ complexes $CpV(CO)_3L$, from Fig. 4, which also contains key references. Table 14 summarizes shift values for, inter alia, various carbonyl-cyclopentadienylvanadium complexes with variations in the Cp system.

Cp complexes of vanadium hold the "world record" on both the highest ^{51}V shielding ($[CpV(CO)_3SnPh_3]^-$: -2059 ppm [113]) and the lowest ^{51}V shielding ($Cp^*_2V_2Te_2Se_2$: $+2375$ ppm [128]; cf. **50b** in Scheme 13 for the structure). Although these two extremes belong to $V^{(I)}$ (d^4) and $V^{(V)}$ (d^0), respectively, the shift value does not unequivocally allow for the specification of the oxidation state of vanadium. As becomes evident on inspection of Table 13 and Fig. 4, the shift ranges for high- and low-valent vanadium complexes clearly overlap.

The ^{51}V nucleus is less shielded in $CpV(CO)_4$ than in the isoelectronic binary

TABLE 13

^{51}V NMR data for half-sandwich complexes of vanadium (V and IV)

Compound	$\delta(^{51}V)$	Other data	Ref.
CpV(N*t*Bu)(O*t*Bu)(*t*Bu) **46**[a]	−465[b]	$W_{1/2}$ 330[b]	105
{CpVO*t*Bu}$_2$(μ-N*t*Bu)$_2$ **47**[a]	−251	$W_{1/2}$ 570	105
CpV(N*t*Bu)XX′			26
X, X′ = O*t*Bu	−904	$W_{1/2}$ 350	
X = O*t*Bu, X′ = Cl	−763	$W_{1/2}$ 400	
X = O*t*Bu, X′ = σ-Cp	−661	$W_{1/2}$ 400	
X, X′ = Cl	−457	$W_{1/2}$ 400	
$CpVOX_2$			
2X = 2 OPh/CH_2Cl_2	−700		106
2 F	−404	J(F,V) 234	108
2 Cl/$CDCl_3$	−403	$W_{1/2}$ 65	107
2 Br/CH_2Cl_2	−249		106
2 SPh/CH_2Cl_2	−204		106
X_2 = $(SC_4H_4)_2Fe$[c] **48a**	+68	$W_{1/2}$ 144	107
$(SeC_4H_4)_2Fe$[c] **48b**	+275	$W_{1/2}$ 158	107
S_5[d]	−46	$W_{1/2}$ 110	109
Cp′$VOCl_2/CH_2Cl_2$	−323		106
Cp*$VOCl_2/CDCl_3$	−25	$W_{1/2}$ 66	107
{Cp*VOX_2}$_2\mu$-O (**49**), X = F	−509	J(F,V) 190	108
Cl	−360	$W_{1/2}$ 250	108
Br	−309	$W_{1/2}$ 295	108
I	−238	$W_{1/2}$ 333	108
Cp*V(O)S_5[d]	+44		109
Cp*$_2V_2S_5$	+596		109
Cp*$_2V_2Se_n$[e] n = 5 **50a**	+1119		110
4 **50b**	+2139		110
3 **50c**	+2205		110

[a] Compound **47**, which is formed from its precursor **46** by β-elimination of isobutene (Scheme 13), contains two V(IV) centres and is diamagnetic despite the rather long d(V–V) = 291 pm.
[b] At 193 K.
[c] 1,1′-Ferrocene dichalcogenate; cf. Scheme 13.
[d] The complex contains the VS_5 ring in the chair conformation.
[e] For mixed species containing O, S, Se and Te, see ref. 111.

carbonyl. This is not always so for other transition metals. The extent to which the shift values of $CpM(CO)_n$ and $M(CO)_m$ deviate, is documented in Table 15.

A marked effect on $\delta(^{51}V)$ is observed as the Cp ring carries substituents. The effect is almost always a deshielding of the ^{51}V nucleus, irrespective of whether the substituent exerts a −M or +M, −I or +I effect. Increasing the electron density in the π system of the Cp ring by gradual increase of methyl substitution gradually decreases shielding. The lowest shielding in this series is consequently observed in Cp* complexes. With one exception, $Cp/Cp^*V(CO)_3SMe_2$ [112], this is the case for

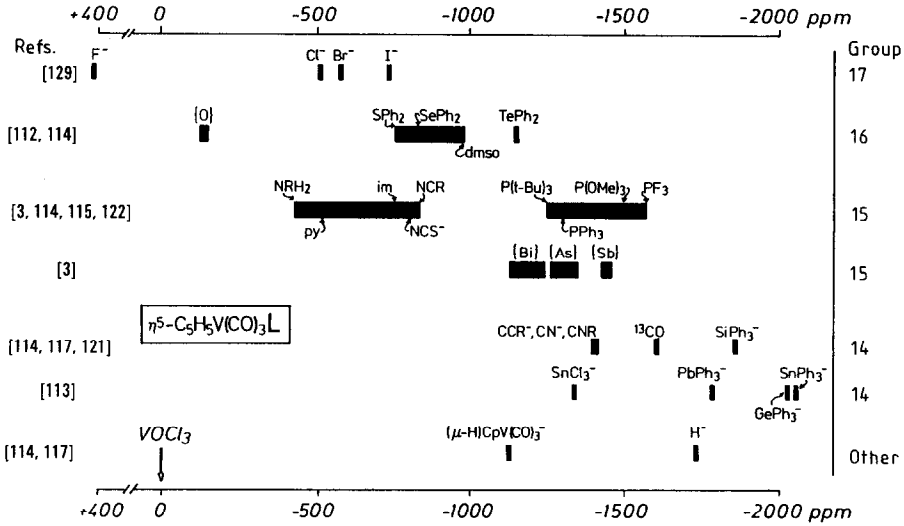

Fig. 4. Schematic representation of the $\delta(^{51}V)$ values for various complexes of composition $C_5H_5V(CO)_3L$. The group numbers for the coordinating ligand functions are noted on the right and key references on the left.

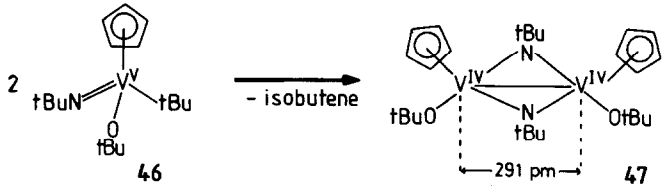

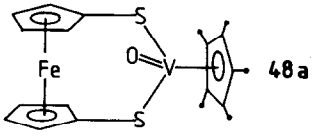

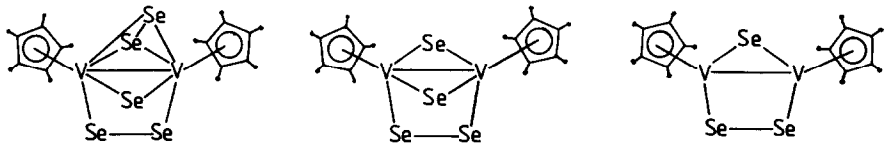

Scheme 13.

TABLE 14

^{51}V NMR data for half-sandwich complexes of carbonylvanadium (III to −I)

Compound	$\delta(^{51}V)$	Other data	Ref.
$Cp^*_2V_2(CO)_4(\mu\text{-}S)_2$	−721	$W_{1/2}$ 1200	112
$Cp^*_2V_2(CO)_4(\mu\text{-}SMe)_2$	−777	$W_{1/2}$ 1235	112
$[CpV(CO)_3SnPh_3]^-$	−2059		113
$[CpV(CO)_3H]^-$	−1730	J(H,V) 22	117
		$^1\Delta^V(^2H)^a$ −6.3	117
$CpV(CO)_4$	−1534	$W_{1/2}$ 15	115
		$J(C_{CO},V)$ 107	117
		NQCC[b] 2.79	11
		η^b 0.11	119
		$^1\Delta^V(^{13}CO)^a$ −0.46	120
		$^2\Delta^V(C^{18}O)^a$ −0.13	120
		$^2\Delta^V(^2H_{Cp})^a$ −0.72	120
		$d\delta/dT^c$ −0.61	118
$[\{CpV(CO)_3\}_2(\mu\text{-}H)]^-$	−1129		114
η^5-$CpV(CO)_4$[d]		$W_{1/2}$[e]	115
Cp = C_5H_5	−1534	See above	
C_5H_4Me	−1525		
$C_5H_3Me_2$	−1515/−1520[f]		
$C_5H_2Me_3$	−1503/−1507[f]		
C_5HMe_4	−1496		
C_5Me_5	−1492		
$C_5H_4(C_7H_{11})$ **51**[g]	−1494		123
C_5H_4(trityl)	−1484	$W_{1/2}$ 350	115
indenyl	−1375		115
fluorenyl	−1118		115
{(Azulene)$V(CO)_4$}$_2$	−1428	$W_{1/2}$ 70	115
{(Acenaphthylene)$V(CO)_4$}$_2$ **52**[h]	−1356/−1347[i]		124
η^5-$CpV(CO)_4$, Cp = $C_5H_4SiMe_3$	−1542	$W_{1/2}$ 40	125
$C_5H_4GeEt_3$	−1555	$W_{1/2}$ 60	125
$C_5H_4SnEt_3$	−1524	$W_{1/2}$ 110	125
$C_5H_4C(O)Me$	−1406	$W_{1/2}$ 10	115
$C_5H_4CH(OH)Me$	−1510		115
$C_5H_4CH(NOH)Me$	−1459		115
C_5Cl_5	−1010	$W_{1/2}$ 20	126
C_5Br_5	−1029	$W_{1/2}$ 20	126
$[\eta^6$-tolV$(CO)_4]^+$	−1660		115
η^7-$TpV(CO)_3$	−1485		115
		NQCC 2.4	116
$Cp_2V_2(CO)_5$	−1664		115
$[\{C_5H_3Me(sBu)\}_2V(CO)_2]^+$	−1115		115

TABLE 14 (*Continued*)

Compound	$\delta(^{51}V)$	Other data	Ref.
$C_5H_4CZ_2V(CO)_3SnPh_3$			123
$Z = NMe_2$ **53a**[j]	−1510		
SCH_2CH_2S **53b**[j]	−1414		
$C_5H_4CH(NMe_2)V(CO)_2NO$ **54**[j]	−1293		123
$CpV(NO)_2CO$	−1294		127

[a] NQCC (MHz) and η (asymmetry parameter) as obtained from a ^{51}V NMR study of a polycrystalline sample.

[b] $^{n}\Delta^{V}(L)$ indicates the *n*-bond isotope effect (ppm) induced on the ^{51}V nucleus by substituting a ligand nucleus by its heavier isotope (e.g. ^{12}C by ^{13}C). The negative sign indicates an upfield shift.

[c] Temperature gradient (ppm deg^{-1}) of the chemical shift. The negative sign indicates an upfield shift as the temperature goes down.

[d] In THF.

[e] Between 20 and 50 Hz, unless indicated otherwise.

[f] The two signals correspond to the two positional isomers.

[g] A cyclic alkenyl-cyclopentadiene; cf. Scheme 14.

[h] See Scheme 14.

[i] The two signals belong to the two *meso* forms (*exo* and *endo*).

[j] There is a more or less pronounced fulvenoid contribution to the resonance hybrid as shown for **53b** and **54** in Scheme 14.

low- and high-valent compounds, and is a general feature for all transition metal nuclei (Table 15). Steric effects have been made responsible for the deshielding in low-valent cyclopentadienylvanadium complexes [115], an argument which appears to be backed up by an additional deshielding in $C_5H_4RV(CO)_4$, if R is a bulky substituent such as Cy or CPh_3 (trityl; Table 14). Increasing steric hindrance leads to diminished metal–ligand overlap, and this in turn should decrease ΔE in eqn. (3), as suggested for $CpMo(CO)_3HgX$, where a similar trend is observed for ^{95}Mo shielding [130].

Ring anellation (indenyl, fluorenyl, azulene, acenaphthylene; for the latter see **52** in Scheme 14) also induces a deshielding of the ^{51}V nucleus.

^{51}V NMR spectroscopy has turned out to be a sensitive tool to probe mixtures of steric isomers. Thus, in the case of the dinuclear acenaphthylene complex **52**, two signals are found in solution, corresponding to the two *meso* forms (*exo-exo* and *endo-endo* linkage of the two halves of the molecule), while only the *exo* isomer has been isolated in the crystalline state [124]. Figure 5 illustrates two other examples of positional and optical isomers. Similar distinctions between diastereomers have been noted for cyclopentadienyl–Mo and tris(pyrazolyl)borato–Mo complexes [132] (vide infra).

TABLE 15

Shift differences $\Delta\delta$ for the pairs $CpM(CO)_n/M(CO)_m$ and $CpM(CO)_n/Cp^*M(CO)_n$

Nucleus	Compounds	$\Delta\delta$[a]
^{49}Ti	$[CpTi(CO)_4]^-/[Ti(CO)_6]^{2-}$	+117
^{51}V	$CpV(CO)_4/[V(CO)_6]^-$	+418
^{93}Nb	$CpNb(CO)_4/[Nb(CO)_6]^-$	+104
^{95}Mo	$[CpMo(CO)_3]^-/Mo(CO)_6$	−266
^{55}Mn	$CpMn(CO)_3/[Mn(CO)_6]^+$	−835
^{57}Fe	$[CpFe(CO)_3]^+/Fe(CO)_5$	+686
^{59}Co	$Cp(Co)(CO)_2/[Co(CO)_4]^-$	+425
^{49}Ti	Cp/Cp^*TiCl_2	−329
^{91}Zr	Cp/Cp^*ZrCl_2	−195
^{51}V	Cp/Cp^*VOCl_2	−378
	Cp/Cp^*VOS_5	−90
	$Cp/Cp^*V(CO)_3SMe_2$	+28
	$Cp/Cp^*V(CO)_4$	−42
^{95}Mo	$Cp/Cp^*Mo(CO)_2NO$	−180
	$Hg[Cp/Cp^*Mo(CO)_3]_2$	−203
^{57}Fe	$Cp(Cp/Cp^*)Fe$	−155
^{59}Co	$Cp/Cp^*Co(1,5\text{-}COD)$	−237
	$Cp/Cp^*Co(C_2H_4)_2$	−235

[a] A negative sign indicates deshielding of the complex named second relative to that named first.

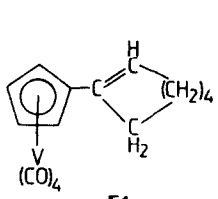

51

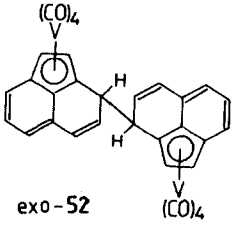

exo-52

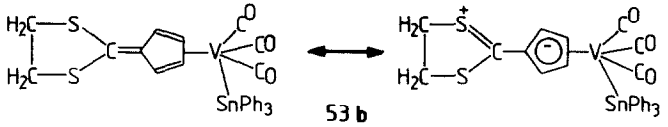

53 b

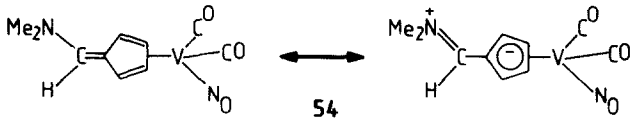

54

Scheme 14.

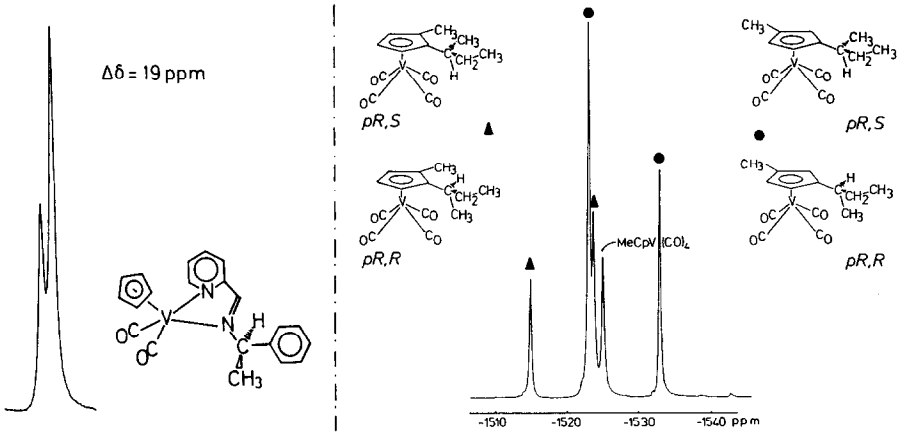

Fig. 5. Left: 32.7 MHz ^{51}V NMR spectrum of the two diastereomeric pairs of enantiomers for a Schiff base derivative of $CpV(CO)_4$, having two centres of chirality (V* and C*) (from ref. 131). Right: 94.6 MHz ^{51}V NMR spectrum of the two positional isomers (marked ▲ and ●) of a $CpV(CO)_4$ derivative carrying two ring substituents. For each of the positional isomers, there are two optical diastereomers arising from a plane of chirality (the Cp ring) and a centre of chirality (the secondary *exo* carbon). $C_5H_4MeV(CO)_4$ has been used as an internal standard (from ref. 124).

(iii) Niobium, molybdenum, tungsten and manganese

Data (Table 16) are mainly available for Mo complexes. The nucleus ^{95}Mo has a rather small quadrupole moment of -0.019×10^{-28} m^2, which allows observation of reasonably sharp signals even in complexes of low point symmetry. The complexes η^6-areneMo(CO)$_3$ give very sharp ^{95}Mo resonances ($W_{1/2}$ ca. 6 Hz), indicative of local C_{3v} symmetry where, in the narrowing of the point-charge model, quadrupole relaxation vanishes. As in Cp compounds, increasing methyl substitution in the arene half-sandwich complexes decreases shielding of the metal nucleus [141] (cf. Table 16). The Mo–arene bond strength decreases in the same direction, again supporting steric arguments for the deshielding effect. A deshielding of 98 ppm has also been noted for (η^6-toluene)$_2$Mo vs. (η^6-benzene)$_2$Mo [84].

Hydrido derivatives of half-sandwich complexes deserve special mention since shielding of the metal nucleus in these compounds is extremely high (Tables 14 and 16 contain examples for ^{51}V, ^{93}Nb, ^{95}Mo and ^{183}W). Similar high shieldings are also induced by germyl, stannyl and plumbyl ligands (while shielding in alkyl complexes is less pronounced than in hydrides). The common origin is the high polarizability of H^- and, for example, SnR_3^- which, as discussed previously for other highly polarizable ligands, gives rise to small factors $C_2\langle r^{-3}\rangle$ in eqn. (3) and hence small paramagnetic deshielding contributions. Another interesting aspect in the context of hybrido complexes is the large deuterium isotope shift of -6 to -11 ppm (i.e. upfield for the heavier isotopomer) of δ(M) (see refs. 118 and 133 for a treatment of this phenomenon and the related temperature effect).

TABLE 16

Data for π arene complexes of Nb, Mo, W and Mn

Compound	δ(M)	Other data	Ref.
$CpNb(CO)_4$/THF	−2017	$\partial\delta/\partial T$[a] −0.36	133
		$J(C_{CO},Nb)$ 236	5
		$J(C_{Cp},Nb)$ ca. 13	5
		$^1\Delta^{Nb}(^{13}C)$[b] −0.373	133
		NQCC[c] 2.26	119
$[CpNbH(CO)_3]^-$	−2252	$W_{1/2}$ 160; $^1\Delta^{Nb}(^2H)$[b] −6	134
$[CpNb(GePh_3)(CO)_3]^-$	−2025	$W_{1/2}$ 10,100	135
$[CpNb(CO)_3\mu\text{-}H(Cr(CO)_5]$ **55a**[d]	−1845	$W_{1/2}$6,100; J(H,Nb) 58	136
$Cp_3Nb_3(CO)_7$ **55b**[d]	−1785[e]		137
Cp_2NbH_3	−2225	T_1 2×10^{-5}	138
$[CpMo(CO)_3]^-$	−2123	$W_{1/2}$ 20	11
$CpMo(CO)_3H$	−2047	$W_{1/2}$ 40	11
$CpMo(CO)_3CH_2Ph$		T_1 4.9; T_2 4.8	11
$Hg[CpMo(CO)_3]_2$, Cp = C_5H_5	−1834	$W_{1/2}$ 160	130
C_5H_4Me	−1795	$W_{1/2}$ 80	130
C_5Me_5	−1631	$W_{1/2}$ 140	130
C_5HPh_4	−1547	$W_{1/2}$ 150	130
$Ph_3PbMo(CO)_3Cp$	−1927	$W_{1/2}$ 180	139
$Ph_2Pb[Mo(CO)_3Cp]_2$	−1838	$W_{1/2}$ 170	139
$[CpMo(CO)_2(NN)]^+$ **56a**[d]	−154/−168[f]		132
$CpMo(CO)_2(N'N)$ **56b**[d]	−293/−310[f]		132
$CpMo(CO)_2(NC)$ **56c**[d]	−383/−396[f]		132
$CpMo(CO)_2NO$	−1584	$J(^{14}N,Mo)$ 46	11
$Cp^*Mo(CO)_2NO$	−1404	$J(^{14}N,Mo)$ 46	11
$CpMo(NO)(SPh)_2$	+144	$W_{1/2}$ 580	140
$CpMo(NO)_2Br$	−883	$W_{1/2}$ 70	11
η^6-areneMo(CO)$_3$			141
arene = tol	−2034		
o-xylene	−1988		
p-xylene	−1979		
m-xylene	−1971		
mes	−1907	T_1 77.6; T_2 55	
$\eta^5{:}\eta^1$-$C_5H_4CMe_2Mo(\eta^6\text{-}C_6H_6)$ **57**[d]	−1923	$W_{1/2}$ 40	84
$(\eta^6$-arene$)_2$Mo			84
arene = benzene	−1362	$W_{1/2}$ 50	
tol	−1270	$W_{1/2}$ 55	
$[(\eta^6\text{-}C_6H_6)(\eta^7\text{-}C_7H_7)Mo]^+$	−487	$W_{1/2}$ 150	84
$[CpW(CO)_3]_2$	−4033		11
$CpW(CO)_3H$	−4010	$^1\Delta^W(^2H)$[b] −11	11
$CpW(CO)_3Me$	−3542		11
$Ph_3PbW(CO)_3Cp$		J(Pb,W) 390	139
$Ph_2Pb[W(CO)_3Cp]_2$		J(Pb,W) 270	139

TABLE 16 (*Continued*)

Compound	δ(M)	Other data	Ref.
$[HW(CO)_3]_2\mu$-$[(C_5H_4)_2SiMe_2]$ **58**[d]	−3982	J(H,W) 36	142
59[d]	−3854	J(H,W) 39; J(P,W) 201	142
$CpMn(CO)_3$	−2280		60

[a] Temperature gradient (ppm deg^{-1}).
[b] Isotope shift (ppm) of $\delta(^{93}Nb)$.
[c] Nuclear quadrupole coupling constant (MHz) obtained from a polycrystalline sample.
[d] See Scheme 15.
[e] $\delta(^{93}Nb)$ has a maximum (1807 ppm) at 310 K, indicating a dynamic component contributing to the shielding.
[f] Two diastereomers.

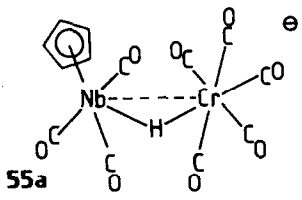

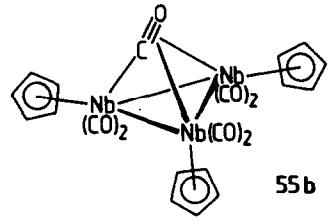

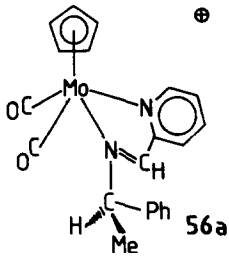

δ -154/-168

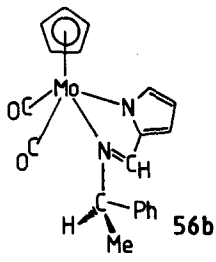

-293/-310

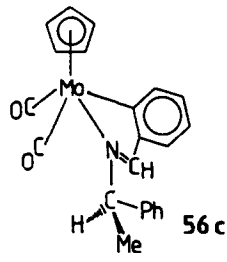

-383/-396

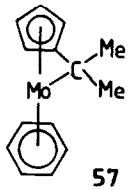

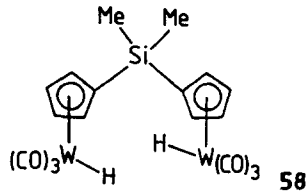

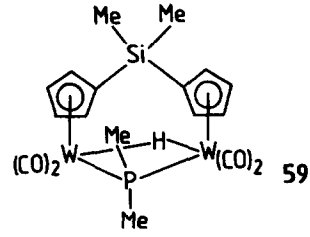

Scheme 15.

$CpNb(CO)_4$ (and also its lighter homologue) have also been the subject of a study under anisotropic conditions [119], viz. in the polycrystalline state, where a second-order quadrupole pattern is observed, and in a nematic liquid crystal, where the NMR spectra reveal a splitting due to first-order quadrupole interaction. (Fig. 6.)

(iv) Iron and osmium

Sandwich and half-sandwich complexes of iron have been probed by direct ^{57}Fe NMR [83,143,144] and indirect, multiple resonance techniques (e.g. $^{13}C\{^{57}Fe\}$ [145], $^{1}H\{^{57}Fe\}$ [146], $^{31}P,^{57}Fe\{^{1}H\}$ [48]). Only an isolated report seems to be available for ^{187}Os, obtained from $^{1}H\{^{187}Os\}$ INEPT measurements of bridged, dinuclear η^6-arene complexes of the type **66** shown in Scheme 16 [147]. Data are collected in Table 17.

Cyclopentadienyl complexes derived from $Fe(CO)_5$ are generally less shielded than corresponding olefin complexes. The trends observed in the ferrocenyl complexes are very much reminiscent of those noted in Sect. (ii) for ring-derivated $CpV(CO)_4$: sp^3 alkyl substitution leads to moderate deshielding of the ^{57}Fe nucleus. The deshielding effect is more pronounced, if the substituent carbon is sp^2 hybridized, and even more so if the sp^2 carbon carries a carbonyl oxygen or is part of a phenyl ring [143].

Protonation ($[Cp_2Fe(H)]^+$) as usual (see above) produces a high-field shift. A high-field shift with respect to ferrocene is also evident in $[CpFeC_5H_4CH_2]^+$, **62** (Scheme 16). **62**, rather than being a ferrocene, is more appropriately described as a complex of composition η^5-$CpFe\eta^6$-$C_5H_4CH_2$, i.e. a fulvenoid coordination of one

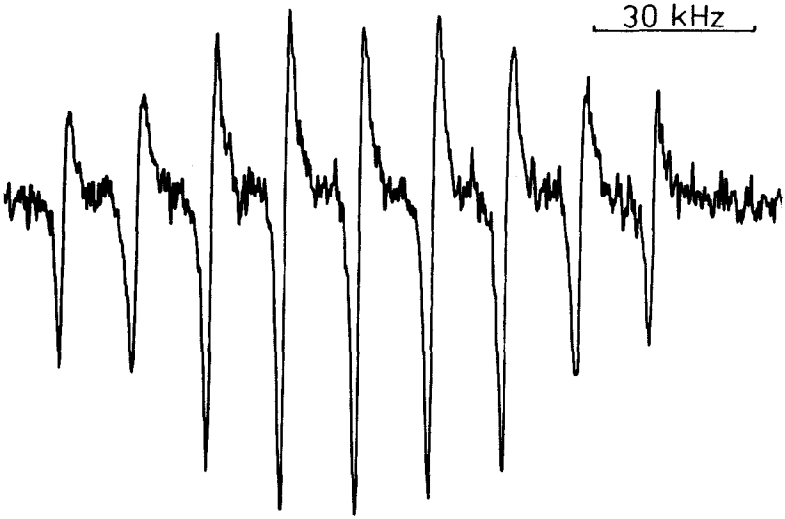

Fig. 6. 16.0 MHz ^{93}Nb NMR spectrum of $CpNb(CO)_4$ dissolved in nematic phase 4, showing the quadrupole splitting into nine equidistant components for the spin 9/2 nucleus ^{93}Nb [119]. The ordering factor is 0.30.

TABLE 17

NMR data for iron and osmium complexes containing π-arene ligands

Compound[a]	δ(M)	Other data	Ref.
$[Cp_2FeH]^+$	+429		145
$[FcCH_2][HSO_4]$ **62**	+1015	J(C,Fe) 0.8–4.4	145
Ferrocenophane **60**	+1263	J(C,Fe) 4.4, 4.8	145
$FcCH_2OH$	+1542		143
FcH (=ferrocene)	+1543	J(C,Fe) 4.8	143
FcMe	+1583		145
FcC≡CH	+1685		143
$FcCH{\equiv}CH_2$	+1709		143
FcPh	+1731		143
FcC(O)Me	+1777		143
$FcC(O)C_5H_4Mn(CO)_3$ **61**	+1810		145
$[FcCHC_5H_4Mn(CO)_3][O_2CCF_3]$	+1908		145
$[CpFe(\eta^6\text{-benzene})]^+$	+1571	J(C,Fe) 3.3, 4.8	145
Cp*FeCp	+1698		144
$(\eta^5\text{-2,3-Me}_2\text{-pentadienyl})_2Fe$ **63**	+2169/+2236[c]		144
$(\eta^5\text{-2,4-Me}_2\text{-pentadienyl})FeCp$	+2277		144
$(\eta^5\text{-Indenyl})_2Fe$	+2500		144
$(\eta^5\text{-Phospha-Cp})_2Fe$ **64**[c]	+1897/+1923	J(P,Fe) ca.16	1
$(\eta^4\text{-Dipohosphacybu})Fe(CO)_3$ **65**	−557	J(P,Fe) 10	48
$(\eta^4\text{-Cyclobutadiene})Fe(CO)_3$	−583	$J(C_{CO},Fe)$ 28.7	83
$Cp_2Fe_2(CO)_4$ **66**	+359		145
$[CpFe(CO)_3]^+$	+686		144
$[TpFe(CO)_2]^+$	+1435		1
CpFe(H)dppe	+832		146
$[\{(\eta^6\text{-arene})Os\}_2(\mu\text{-H})_3]^+$ **67**	−2526	J(H,Os) 84	147
$[\{(\eta^6\text{-arene})Os(\mu\text{-H})\}_4]^{2+}$	−2171	J(H,Os) 36	147
$[\{(\eta^6\text{-arene})Os\}_2(\mu\text{-H})_2(\mu\text{-Ac})]^+$	−1185	J(H,Os) 76	147

[a] Fc stands for ferrocenyl (η^5-$C_5H_5Fe\eta^5$-C_5H_4). See Scheme 16 for numbered complexes.
[b] Two diastereomers.

of the five rings [145], a view which is supported by the size of the coupling constants $J(^{13}C-^{57}Fe)$ for **62**. Compare also the Cp–vanadium complexes **53b** and **54** (Scheme 14) where fulvenoid coordination participates.

The diastereomers in the unsymmetrically substituted bis(η^5-pentadienyl) complexes **63** and the bis(η^5-phosphacyclopentadienyl) complexes **64** are distinguished by their $\delta(^{57}Fe)$ values (Table 17). Both (η^4-cyclobutadiene)$Fe(CO)_3$ and (η^4-1,3-diphosphacyclobutadiene)$Fe(CO)_3$ (**65**) give rise to extreme ^{57}Fe shielding, a feature which is also observed, as far as the cyclobutadiene complexes are concerned, in the corresponding Co and Rh compounds. There is a consistent decrease of shielding in

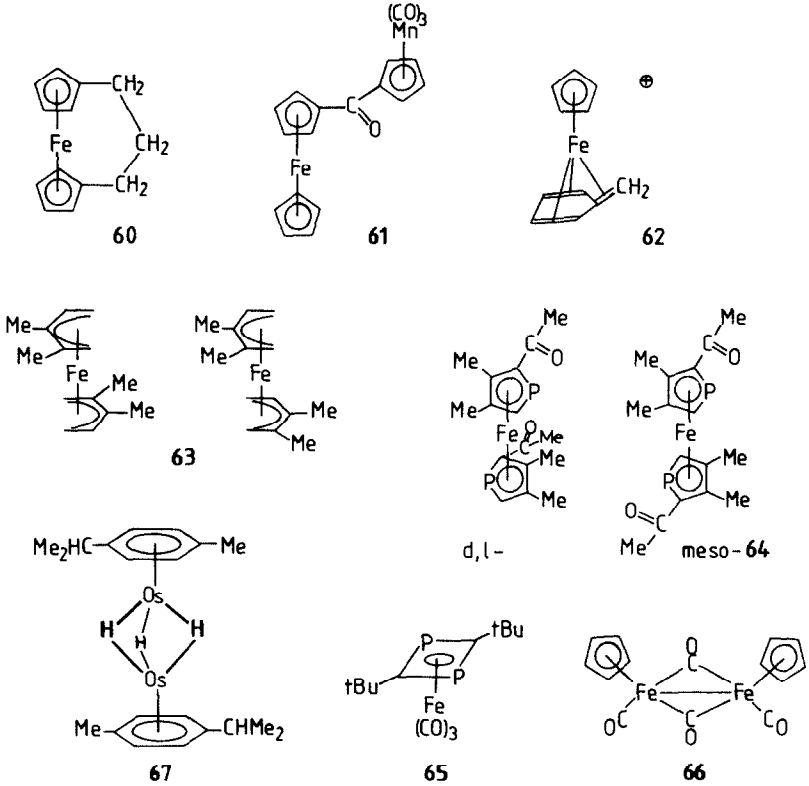

Scheme 16.

the $\{(\eta^n\text{-arene})Fe(CO)_m\}$ complexes passing from η^4-C_4H_4 to η^5-C_5H_5 and further to η^7-C_7H_7.

(v) Cobalt and rhodium. The relationship between catalytic activity and $\delta(^{59}Co)$

The catalytic activity of η^5-$(C_5H_4Z)Co$(diene) complexes in the co-trimerization of alkynes and nitriles (formation of pyridines) has been shown to be closely connected to the ^{59}Co chemical shifts as correlated to the substituent Z [86]. The reaction is shown in Scheme 17. The first step is the elimination (at temperatures of 100–250 °C) of the diene, preferably 1,5-COD. The corresponding cyclobutadiene complex does not readily form a catalytic active species, supporting, along with the unusually high metal shielding it induces, its aromatic (6-π electron donating) character. Once the $(C_5H_4R)Co$ moeity is initiated, the catalysis is independent of the olefin originally attached to Co. There is a close relationship between $\delta(^{59}Co)$ and the regioselectivity of product (pyridine) formation. With increasing ^{59}Co shielding (Table 18), the amount of the symmetrical isomer **a** increases at the expense of the unsymmetrical

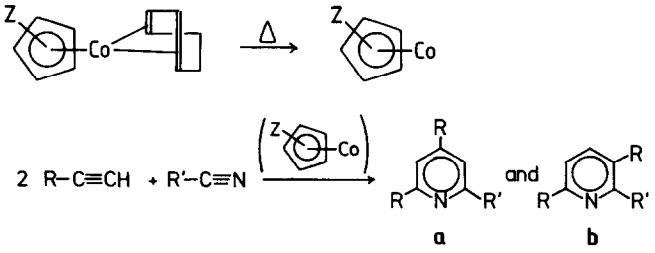

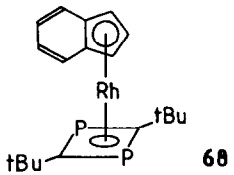

Scheme 17.

TABLE 18

Data for π-arene cobalt and rhodium complexes

Compound	δ(M)	Other data	Ref.
η^4-C_4H_4Co(1,5-COD)	−2888		86(a)
$CpCo(CO)_2$	−2675		148
η^5-CpCo(1,5-COD)[a]			86(a)
η^5-Cp = C_5Me_5	−1413		
C_5H_3cyclo-$(CH_2)_3$	−1261	$W_{1/2}$ 8,400	
C_5H_4Me	−1227		
C_5H_5	−1176	$W_{1/2}$ 6,300	
C_5H_4tBu	−1166		
$C_5H_4SiMe_3$	−1149	$W_{1/2}$ 11,100	
C_5H_4Ph	−1088		
$C_5H_4C(O)Me$	−1055		
Indenyl	−861	$W_{1/2}$ 7,700	87
$Cp^*Co(C_2H_4)_2$	−1490	$W_{1/2}$ 9,900	87
$CpCo(C_2H_4)_2$	−1235	$W_{1/2}$ 6,800	87
η^4-$C_4H_4Rh(Cp)$	−10831	J(C,Rh) 11.7	18
$[Cp_2Rh]Cl$	−10613		18
(η^5-Ind)Rh(diphosphacybu) **68**	−10216	J(P,Rh) 31.3	38
$CpRh(CO)_2$	−10096		18

[a] Slightly differing δ values are reported in ref. 87.

isomer **b** (Scheme 17). Thus, the largest amount of isomer **a** is observed for {Cp*Co}, while **b** is the main isomer if acetyl-Cp is the catalytic active species.

The shielding pattern is equal to those discussed in the previous sections. The high shielding of the ^{59}Co nucleus in $CpCo(CO)_2$ (−2675) as compared with that in $CpCo(C_2H_4)_2$ (−1235) has been rationalized in terms of the larger (by 0.3 eV) HOMO–LUMO gap and the smaller Co–LCAO coefficient(s) of the LUMO for the dicarbonyl species [87], giving rise to a less effective σ'(para) in eqn. (3).

REFERENCES

1 W. von Philipsborn, Pure Appl. Chem., 58 (1986) 513.
2 R. Benn and A. Rufińska, Angew. Chem., 24 (1986) 861.
3 D. Rehder, Magn. Reson. Rev., 9 (1984) 125.
4 J.J. Dechter, Prog. Inorg. Chem., 33 (1985) 393.
5 D. Rehder, Chimia, 40 (1986) 198.
6 J. Mason, Chem. Rev., 87 (1987) 1299.
7 J. Mason, Polyhedron, 8 (1989) 1657.
8 N. Juranić, Coord. Chem. Rev., 96 (1989) 253.
9 K. Kanda, H. Nakatsuji and T. Yonezawa, J. Am. Chem. Soc., 106 (1984) 5888.
10 (a) D. Rehder, Bull. Magn. Reson., 4 (1982) 33.
(b) O.W. Howarth, Prog. Nucl. Magn. Reson. Spectrosc., 22 (1990) 453.
11 M. Minelli, J.H. Enemark, R.T.C. Brownlee, M.J. O'Connor and A.G. Wedd, Coord. Chem. Rev., 68 (1985) 169.
12 P.S. Pregosin, Ann. Rep. NMR Spectrosc., 17 (1986) 285.
13 P. Laszlo (Ed.), NMR of Newly Accessible Nuclei, Academic Press, New York, 1983.
14 J. Mason (Ed.), Multinuclear NMR, Plenum Press, New York, 1987.
15 P.S. Pregosin (Ed.), Transition Metal NMR, Elsevier, Amsterdam, 1991, in press.
16 J.W. Akitt and W.S. McDonald, J. Magn. Reson., 58 (1984) 401.
17 R. Bonnaire, D. Davoust and N. Platzer, Org. Magn. Reson., 22 (1984) 80.
18 E. Maurer, S. Rieker, M. Schollbach, A. Schwenk, T. Egolf and W. von Philipsborn, Helv. Chim. Acta, 65 (1982) 26.
19 W.J. Evans, J.M. Meadows, A.G. Kostka and G.L. Closs, Organometallics, 4 (1985) 324.
20 S.H. Eggers, M. Adam, E.T.K. Haupt and R.D. Fischer, Inorg. Chim. Acta, 39 (1987) 315.
21 M. Adam, E.T.K. Haupt and R.D. Fischer, Bull. Magn. Reson., 12 (1990) 101.
22 S. Berger, W. Bock, C.F. Marth, B. Raguse and M.T. Reetz, Magn. Reson. Chem., 28 (1990) 559.
23 R. Benn and A. Rufińska, J. Organomet. Chem., 273 (1984) C51.
24 W.A. Herrman, G. Weichselbaumer and H.J. Kneuper, J. Organomet. Chem., 319 (1987) C21.
25 F. Preuss, H. Becker and T. Wieland, Z. Naturforsch. Teil B, 45 (1990) 191.
26 F. Preuss, H. Becker and H.-J. Häusler, Z. Naturforsch. Teil B, 42 (1987) 881.
27 F. Preuss and H. Becker, Z. Naturforsch. Teil B, 41 (1986) 185.
28 D.D. Devore, J.D. Lichtenhan, F. Takusagawa and E.A. Maatta, J. Am. Chem. Soc., 109 (1987) 7408.
29 J. de With, A.D. Horton and A.G. Orpen, Organometallics, 9 (1990) 2207.
30 F. Süssmilch, W. Glöckner and D. Rehder, J. Organomet. Chem., 388 (1990) 95.
31 D. Rehder, C. Weidemann, A. Duch and W. Priebsch, Inorg. Chem., 27 (1988) 584.
32 H. Nakatsuji and M. Sugimoto, Inorg. Chem., 29 (1990) 1221.

H. Nakatsuji, M. Sugimoto and S. Saito, Inorg. Chem., 29 (1990) 3095.
33 A. Hafner, L.S. Hegedus, G. deWeck, B. Hawkins and K.H. Dötz, J. Am. Chem. Soc., 110 (1988) 8413.
34 J.Y. LeGall, M.M. Kubicki and F.Y. Petillon, J. Organomet. Chem., 221 (1981) 287.
35 R.T.C. Brownlee, A.F. Masters, M.J. O'Connor, A.G. Wedd, H.A. Kimlin and J.D. Cotton, Org. Magn. Reson., 20 (1982) 73.
J.D. Cotton, R.D. Markwell, Inorg. Chim. Acta, 175 (1990) 187.
36 R. Benn, A. Rufińska, M.A. King, C.E. Osterberg and T.G. Richmond, J. Organomet. Chem., 376 (1989) 359.
37 C.G. Young, E.M. Kober and J.H. Enemark, Polyhedron, 6 (1987) 255.
38 R. Benn and A. Rufińska, Magn. Reson. Chem., 26 (1988) 895.
39 C.G. Young and J.H. Enemark, Aust. J. Chem., 39 (1986) 997.
40 J.D. Cotton and R.D. Markwell, Inorg. Chim. Acta, 175 (1990) 187.
41 P. Oltmanns and D. Rehder, J. Organomet. Chem., 281 (1985) 263.
42 P. DeShong, G.A. Slough, D.R. Sidler, P.J. Rybczynski, W. von Philipsborn, R.W. Kunz, B.E. Bursten and T.W. Clayton, Jr., Organometallics, 8 (1989) 1381.
43 P. DeShong, D.R. Sidler, P.J. Rybczynski, A.A. Ogilvie and W. von Philipsborn, J. Org. Chem., 54 (1989) 5432.
44 A.P. Masters and T.S. Sorensen, Can. J. Chem., 68 (1990) 492.
45 J. Chung, H.C. Lee and E. Oldfield, J. Magn. Reson., 90 (1990) 148.
46 (a) L. Baltzer, J. Am. Chem. Soc., 109 (1987) 3479.
(b) G.N. La Mar, C.M. Dellinger and S.S. Sankar, Biochem. Biophys. Res. Commun., 128 (1985) 628.
47 E. Maurer, S. Rieker, M. Schollbach, A. Schwenk, T. Egolf and W. von Philipsborn, Helv. Chim. Acta, 65 (1982) 26.
48 R. Benn, H. Brenneke, A. Frings, H. Lehmkuhl, G. Mehler, A. Rufińska and T. Wildt, J. Am. Chem. Soc., 110 (1988) 5661.
49 R. Benn, H. Brenneke, E. Joussen, H. Lehmkuhl and F. Lopez Ortiz, Organometallics, 9 (1990) 756.
50 R. Benn, H. Brenneke and A. Rufińska, J. Organomet. Chem., 320 (1987) 115.
51 C. Crocker, R.J. Errington, R. Markham, C.J. Moulton, K.J. Odell and B.L. Shaw, J. Am. Chem. Soc., 102 (1980) 4373; J. Chem. Soc. Dalton Trans., (1982) 387.
52 C.S. Creaser and J.A. Creighton, J. Organomet. Chem., 157 (1978) 243.
53 N.H. Agnew, T.G. Appleton and J.R. Hall, Aust. J. Chem., 35 (1982) 881.
54 E.W. Abel, T.P.J. Coston, K.G. Orrell and V. Sik, J. Chem. Soc. Dalton Trans., (1990) 49.
55 S. Hietkamp, D. Stufkens and K. Vrieze, J. Organomet. Chem., 169 (1979) 107.
56 A. Sebald, B. Wrackmeyer and W. Beck, Z. Naturforsch. Tiel B., 38 (1983) 45.
57 S.M. Baxter, G.S. Ferguson and T. Wolkzanski, J. Am. Chem. Soc., 110 (1988) 4231.
58 R.K. Harris, P. Reams and K.J. Packer, J. Chem. Soc. Dalton Trans., (1986) 1015.
59 P. Pyykkö, Adv. Quantum Chem., 11 (1978) 353.
60 D. Rehder, H.-Ch. Bechthold, A. Keçeci, H. Schmidt and M. Siewing, Z. Naturforsch. Teil B, 37 (1982) 631.
61 N. Juranić, J. Chem. Soc. Dalton Trans., (1988) 79.
62 A.D. Cardin, P.D. Ellis, J.D. Odom and J.W. Howard, J. Am. Chem. Soc., 97 (1975) 1672.
63 M.A. Sens, N.K. Wilson, P.D. Ellis and J.D. Odom, J. Magn. Reson., 19 (1975) 323.
64 H. Nakatsuji, K. Kanda, K. Endo and T. Yonezawa, J. Am. Chem. Soc., 106 (1984) 4653.
65 J.D. Kennedy, W.J. McFarlane, J. Chem. Soc. Perkin Trans., 2 (1977) 1187.
66 M.J. Albright, A.K. Schaaf and A.J. Hovland, J. Organomet. Chem., 259 (1983) 37.
67 M. Borzo and G.E. Maciel, J. Magn. Reson., 19 (1975) 279.

68 A.R. Norris and R. Kumar, Inorg. Chim. Acta, 93 (1984) L63.
69 M.M. Kubicki, R. Kergoat, J.E. Guerchais, I. Bkouche-Waksman, C. Bois and P. L'Haridon, J. Organomet. Chem., 219 (1981) 329.
70 E. Block, M. Brito, M. Gernon, D. McGowty, H. Kang and J. Zubieta, Inorg. Chem., 29 (1990) 3172.
71 R.G. Kidd and R.J. Goodfellow, in R.K. Harris and B.E. Mann (Eds.), NMR and the Periodic Table, Academic Press, London, 1978, p. 271.
72 J. Eichbichler and P. Peringer, Inorg. Chim. Acta, 43 (1980) 121.
73 T.S. Lobana and M.J.K. Sandhu, Indian J. Chem., 29A (1990) 394.
74 D.K. Breitinger, W. Kress, R. Sendelbeck and K. Ishiwada, J. Organomet. Chem., 243 (1983) 245.
75 A. Sebald and B. Wrackmeyer, Spectrochim. Acta Part A, 38 (1982) 163.
76 G.N. Howell, M.J. O'Connor, A.M. Bond, H.A. Hudson, P.J. Hanna and S. Strother, Aust. J. Chem., 39 (1986) 1167.
77 M. Delnomdedieu, D. Georgescauld, A. Boudou and E.J. Dufourc, Bull. Magn. Reson., 11 (1989) 420.
78 (a) H.G. Alt, H.E. Engelhardt, A. Razavi, M.D. Rausch and R.D. Rogers, Z. Naturforsch. Teil B, 43 (1988) 438.
(b) H.G. Alt and H.E. Engelhardt, Z. Naturforsch. Teil B, 40 (1985) 1134.
79 D. Rehder, cited in B. Bachmann, F. Hahn, J. Heck and M. Wünsch, Organometallics, 8 (1989) 2533.
80 C.J. Jameson, D. Rehder and M. Hoch, J. Am. Chem. Soc., 109 (1987) 2589.
81 K. Ihmels and D. Rehder, Chem. Ber., 118 (1985) 895.
82 R. Benn, C. Brevard, A. Rufińska and G. Schroth, Organometallics, 6 (1987) 938.
83 T. Jenny, W. von Philipsborn, J. Kronenbitter and A. Schenk, J. Organomet. Chem., 205 (1981) 211.
84 J.C. Green, R.A. Grieves and J. Mason, J. Chem. Soc. Dalton Trans., (1986) 1313.
85 R. Benn, E. Joussen, H. Lehmkuhl, F. Lopez Ortiz and A. Rufińska, J. Am. Chem. Soc., 111 (1989) 8754.
86 (a) H. Bönnemann, W. Brijoux, R. Brinkmann, W. Meures and R. Mynott, J. Organomet. Chem., 272 (1984) 231.
(b) H. Bönnemann and W. Brijoux, Bull. Soc. Chim. Belg., 94 (1985) 635.
(c) H. Bönnemann and W. Brijoux, New J. Chem., 11 (1987) 549.
87 R. Benn, K. Cibura, P. Hofmann, K. Jonas and A. Rufinska, Organometallics, 4 (1985) 2214.
88 R. Benn, R.-D. Reinhardt and A. Rufińska, J. Organomet. Chem., 282 (1985) 291.
89 A. Albinati, W.R. Caseri and P.S. Pregosin, Organometallics, 6 (1987) 788.
90 W. Caseri and P.S. Pregosin, Organometallics, 7 (1988) 1373.
91 P.S. Pregosin, Coord. Chem. Rev., 44 (1982) 247.
92 I.M. Al-Najjar and H.B. Amin, J. Chem. Soc. Dalton Trans., (1990) 429.
93 P. Salvadori, G. Uccello-Barretta, R. Lazzaroni and A.M. Caporusso, J. Chem. Soc. Chem. Commun., (1990) 1121.
94 J. Schiemann and E. Weiss, J. Organomet. Chem., 255 (1983) 179.
95 J.W. Faller and B.C. Whitmore, Organometallics, 5 (1986) 752.
96 (a) J. Schiemann, E. Weiss, F. Näumann and D. Rehder, J. Organomet. Chem., 232 (1982) 219.
(b) F. Näumann, D. Rehder and V. Pank, Inorg. Chim. Acta, 84 (1984) 117.
97 A. Ammann, P.S. Pregosin, H. Rüegger, M. Grassi and A. Musco, Magn. Reson. Chem., 27 (1989) 355.

98 A. Musco, R. Pontellini, M. Grassi, A. Sironi, S.V. Meille, H. Rüegger, C. Ammann and P.S. Pregosin, Organometallics, 7 (1988) 2130.
99 P. Bougeard, M. Mancini, B.G. Sayer and J. McGlinchey, Inorg. Chem., 24 (1985) 93.
100 S.H. Eggers and R.D. Fischer, J. Organomet. Chem., 315 (1986) C61.
101 A.G. Avent, M.A. Edelman, M.F. Lappert and G.A. Lawless, J. Am. Chem. Soc., 111 (1989) 3423.
102 K.M. Chi, S.R. Frerichs, S.B. Philson and J.E. Ellis, J. Am. Chem. Soc., 110 (1988) 303.
103 N. Hao, B.G. Sayer, G. Dénès, D.G. Bickley, C. Detellier and M.J. McGlinchey, J. Magn. Reson., 50 (1982) 50.
104 A. Dormond, M. Fauconet, J.C. Leblanc and C. Moise, Polyhedron, 3 (1984) 897.
105 F. Preuss, H. Becker, J. Kaub and W.S. Sheldrick, Z. Naturforsch. Teil B, 43 (1988) 1195.
106 W.A. Herrmann, E. Herdtweck and G. Weichselbaumer, J. Organomet. Chem., 362 (1989) 321.
107 M. Herberhold, M. Schrepfermann and A.L. Rheingold, J. Organomet. Chem., 394 (1990) 113.
108 M. Herberhold, W. Kremnitz, M. Kuhnlein, M.L. Ziegler and K. Brunn, Z. Naturforsch. Teil B, 42 (1987) 1520.
109 M. Herberhold, M. Kuhnlein, M.L. Ziegler and B. Nuber, J. Organomet. Chem., 349 (1988) 131.
110 M. Herberhold and M. Kuhnlein, New J. Chem., 12 (1988) 357.
111 M. Herberhold, M. Kuhnlein, M. Schrepfermann, M.L. Ziegler and B. Nuber, J. Organomet. Chem., 398 (1990) 259.
112 M. Herberhold, M. Kuhnlein, W. Kremitz and A.L. Rheingold, J. Organomet. Chem., 383 (1990) 71.
113 R. Talay and D. Rehder, J. Organomet. Chem., 262 (1984) 25.
114 M. Hoch and D. Rehder, J. Organomet. Chem., 288 (1985) C25.
115 M. Hoch and D. Rehder, Chem. Ber., 121 (1988) 1541.
116 G.M. Whitesides and H.L. Mitchell, J. Am. Chem. Soc., 91 (1969) 2245.
117 M. Hoch and D. Rehder, Inorg. Chim. Acta, 111 (1986) L13.
118 C.J. Jameson, D. Rehder and M. Hoch, J. Am. Chem. Soc., 109 (1987) 3589.
119 D. Rehder, K. Paulsen and W. Basler, J. Magn. Reson., 53 (1983) 500.
120 D. Rehder, M. Hoch and C.J. Jameson, Magn. Reson. Chem., 28 (1990) 138.
121 N.J. Coville, G.W. Harris and D. Rehder, J. Organomet. Chem., 293 (1985) 365.
122 C. Woitha and D. Rehder, J. Organomet. Chem., 353 (1988) 315.
123 D. Rehder and D. Wenke, J. Organomet. Chem., 348 (1988) 205.
124 D. Rehder, M. Hoch and M. Link, Organometallics, 7 (1988) 233.
125 A, Duch, M. Hoch and D. Rehder, Chimia, 42 (1988) 179.
126 W. Priebsch, M. Hoch and D. Rehder, Chem. Ber., 121 (1988) 1971.
127 F. Näumann and D. Rehder, J. Organomet. Chem., 204 (1981) 411.
128 M. Herberhold, personal communication, 1991.
129 R. Talay and D. Rehder, Inorg. Chim. Acta, 77 (1983) L175.
130 M.M. Kubicki, J.Y. Le Gall, R. Pichon, J.Y. Salaun, M. Cano and J.A. Campo, J. Organomet. Chem., 348 (1988) 349.
131 M. Hoch and D. Rehder, Inorg. Chim. Acta, 115 (1986) L23.
132 H. Brunner, P. Beier, E. Frauendorfer, M. Muschiol, D.K. Rastogi, J. Wachter, M. Minelli and J.H. Enemark, Inorg. Chim. Acta, 96 (1985) L5,
133 C.J. Jameson, D. Rehder and M. Hoch, Inorg. Chem., 27 (1988) 3490.
134 F. Näumann, D. Rehder and V. Pank. J. Organomet. Chem., 240 (1982) 363.
135 I. Pforr, F. Näumann and D. Rehder, J. Organomet. Chem., 258 (1983) 189.

136 P. Oltmanns and D. Rehder, J. Organomet. Chem., 345 (1988) 87.
137 W.A. Herrmann, H. Biersack, M.L. Ziegler, K. Weidenhammer, R. Siegel and D. Rehder, J. Am. Chem. Soc., 103 (1981) 1692.
138 M.D. Curtis, L.G. Bell and W.M. Butler, Organometallics, 4 (1985) 701.
139 M.M. Kubicki, J.-Y. Le Gall, R. Kergoat and L.C. Gomes de Lima, Can. J. Chem., 65 (1987) 1292.
140 C.G. Young, M. Minelli, J.H. Enemark, J. Hussain, C.J. Jones and J.A. McCleverty, J. Chem. Soc. Dalton Trans., (1987) 619.
141 A.F. Masters, R.T.C. Brownlee, M.J. O'Connor and A.G. Wedd, Inorg. Chem., 20 (1981) 4183.
142 R. Benn, H. Brenneke, J. Heck and A. Rufińska, Inorg. Chem., 26 (1987) 2826.
143 E. Haslinger, W. Robien, K. Schlögl and W. Weissensteiner, J. Organomet. Chem., 218 (1981) C11.
144 R. Benn, A. Rufińska, M.S. Kralik and R.D. Ernst, J. Organomet. Chem., 375 (1989) 115.
145 A.A. Koridze, N.M. Astakhova and P.V. Petrovskii, J. Organomet. Chem., 254 (1983) 345.
146 R. Benn and C. Brevard, J. Am. Chem. Soc., 108 (1986) 5622.
147 J.A. Cabeza, B.E. Mann, P.M. Maitlis and C. Brevard, J. Chem. Soc. Dalton Trans., (1988) 629.
148 E.A.C. Lucken, K. Noack and D.F. Williams, J. Chem. Soc. A, (1967) 148.